



A Compliant Mechanism Synthesis Theory for Fostering Innovation of Micro Air Vehicles

Haijun Su
OHIO STATE UNIVERSITY THE

04/01/2016
Final Report

DISTRIBUTION A: Distribution approved for public release.

Air Force Research Laboratory
AF Office Of Scientific Research (AFOSR)/ RTA1
Arlington, Virginia 22203
Air Force Materiel Command

REPORT DOCUMENTATION PAGE				<i>Form Approved</i> OMB No. 0704-0188	
<small>The public reporting burden for this collection of information is estimated to average 1 hour per response, including the time for reviewing instructions, searching existing data sources, gathering and maintaining the data needed, and completing and reviewing the collection of information. Send comments regarding this burden estimate or any other aspect of this collection of information, including suggestions for reducing the burden, to the Department of Defense, Executive Service Directorate (0704-0188). Respondents should be aware that notwithstanding any other provision of law, no person shall be subject to any penalty for failing to comply with a collection of information if it does not display a currently valid OMB control number.</small>					
PLEASE DO NOT RETURN YOUR FORM TO THE ABOVE ORGANIZATION.					
1. REPORT DATE (DD-MM-YYYY) 07-30-2016		2. REPORT TYPE Final Report		3. DATES COVERED (From - To) April 2012- March 2016	
4. TITLE AND SUBTITLE A compliant mechanism synthesis theory for fostering innovation of micro air vehicles				5a. CONTRACT NUMBER	
				5b. GRANT NUMBER FA9550-12-1-0070	
				5c. PROGRAM ELEMENT NUMBER	
6. AUTHOR(S) Haijun Su				5d. PROJECT NUMBER	
				5e. TASK NUMBER	
				5f. WORK UNIT NUMBER	
7. PERFORMING ORGANIZATION NAME(S) AND ADDRESS(ES) The Ohio State University Department of Mechanical and Aerospace Engineering 201 W. 19th Ave, Columbus, Ohio 43210				8. PERFORMING ORGANIZATION REPORT NUMBER	
9. SPONSORING/MONITORING AGENCY NAME(S) AND ADDRESS(ES) Air Force Office of Scientific Research 875 North Randolph Street, Suite 325, Room 3112, Arlington, VA., 22203-1768				10. SPONSOR/MONITOR'S ACRONYM(S) AFOSR	
				11. SPONSOR/MONITOR'S REPORT NUMBER(S)	
12. DISTRIBUTION/AVAILABILITY STATEMENT DISTRIBUTION A					
13. SUPPLEMENTARY NOTES					
14. ABSTRACT In this project, we have developed a compliant mechanism synthesis theory that incorporate a general framework for determining pseudo-rigid-body models, type synthesis algorithms (determining mechanism topology for a specific task) and kinetostatic analysis/synthesis. This theory has been implemented into computer codes with a graphical user interface. It has been applied to solve several structure design problems including design optimization of compliant transmission mechanism for flapping wing MAVs, a bistable buckling beam design and a robotic finger actuated using shape memory alloy actuators. For instance, we have developed a parameter optimization framework for determining the pseudo-rigid-body (PRB) model of cantilever beams. A novel concept of "PRB matrix" has been proposed to describe the general topology of an arbitrary PRB model. Based upon this synthesis theory, we have shown that compliant joints can significantly reduce the power consumption in flapping wing MAVs if they are designed to enhance the down stroke flapping motion.					
15. SUBJECT TERMS					
16. SECURITY CLASSIFICATION OF:			17. LIMITATION OF ABSTRACT	18. NUMBER OF PAGES	19a. NAME OF RESPONSIBLE PERSON
a. REPORT	b. ABSTRACT	c. THIS PAGE			19b. TELEPHONE NUMBER (Include area code)

INSTRUCTIONS FOR COMPLETING SF 298

1. REPORT DATE. Full publication date, including day, month, if available. Must cite at least the year and be Year 2000 compliant, e.g. 30-06-1998; xx-06-1998; xx-xx-1998.

2. REPORT TYPE. State the type of report, such as final, technical, interim, memorandum, master's thesis, progress, quarterly, research, special, group study, etc.

3. DATES COVERED. Indicate the time during which the work was performed and the report was written, e.g., Jun 1997 - Jun 1998; 1-10 Jun 1996; May - Nov 1998; Nov 1998.

4. TITLE. Enter title and subtitle with volume number and part number, if applicable. On classified documents, enter the title classification in parentheses.

5a. CONTRACT NUMBER. Enter all contract numbers as they appear in the report, e.g. F33615-86-C-5169.

5b. GRANT NUMBER. Enter all grant numbers as they appear in the report, e.g. AFOSR-82-1234.

5c. PROGRAM ELEMENT NUMBER. Enter all program element numbers as they appear in the report, e.g. 61101A.

5d. PROJECT NUMBER. Enter all project numbers as they appear in the report, e.g. 1F665702D1257; ILIR.

5e. TASK NUMBER. Enter all task numbers as they appear in the report, e.g. 05; RF0330201; T4112.

5f. WORK UNIT NUMBER. Enter all work unit numbers as they appear in the report, e.g. 001; AFAPL30480105.

6. AUTHOR(S). Enter name(s) of person(s) responsible for writing the report, performing the research, or credited with the content of the report. The form of entry is the last name, first name, middle initial, and additional qualifiers separated by commas, e.g. Smith, Richard, J, Jr.

7. PERFORMING ORGANIZATION NAME(S) AND ADDRESS(ES). Self-explanatory.

8. PERFORMING ORGANIZATION REPORT NUMBER. Enter all unique alphanumeric report numbers assigned by the performing organization, e.g. BRL-1234; AFWL-TR-85-4017-Vol-21-PT-2.

9. SPONSORING/MONITORING AGENCY NAME(S) AND ADDRESS(ES). Enter the name and address of the organization(s) financially responsible for and monitoring the work.

10. SPONSOR/MONITOR'S ACRONYM(S). Enter, if available, e.g. BRL, ARDEC, NADC.

11. SPONSOR/MONITOR'S REPORT NUMBER(S). Enter report number as assigned by the sponsoring/monitoring agency, if available, e.g. BRL-TR-829; -215.

12. DISTRIBUTION/AVAILABILITY STATEMENT. Use agency-mandated availability statements to indicate the public availability or distribution limitations of the report. If additional limitations/ restrictions or special markings are indicated, follow agency authorization procedures, e.g. RD/FRD, PROPIN, ITAR, etc. Include copyright information.

13. SUPPLEMENTARY NOTES. Enter information not included elsewhere such as: prepared in cooperation with; translation of; report supersedes; old edition number, etc.

14. ABSTRACT. A brief (approximately 200 words) factual summary of the most significant information.

15. SUBJECT TERMS. Key words or phrases identifying major concepts in the report.

16. SECURITY CLASSIFICATION. Enter security classification in accordance with security classification regulations, e.g. U, C, S, etc. If this form contains classified information, stamp classification level on the top and bottom of this page.

17. LIMITATION OF ABSTRACT. This block must be completed to assign a distribution limitation to the abstract. Enter UU (Unclassified Unlimited) or SAR (Same as Report). An entry in this block is necessary if the abstract is to be limited.

Report Summary

In this project, we have developed a compliant mechanism synthesis theory that incorporate a general framework for determining pseudo-rigid-body models, type synthesis algorithms (determining mechanism topology for a specific task), kinetostatic analysis/synthesis. This research starts from classification and type synthesis of flapping wing MAVs. We have studied over 15 flapping mechanisms in the literature and classify them based on workspace type, linkage topology, rigid body or compliant, actuator type and mobility. This classification lays out the foundation for type synthesis of flapping wing mechanisms. We have also developed a parameter optimization framework for determining the pseudo-rigid-body (PRB) model of cantilever beams. A novel concept of PRB matrix has been proposed to describe the general topology of an arbitrary PRB model. A novel 3-spring pseudo-rigid-body model for soft joints with significant extension effects was proposed. These soft joints are often used in transmission mechanisms in flapping wing micro-air vehicles. Based upon this synthesis theory, we have shown that compliant joints can significantly reduce the power consumption in flapping wing MAVs if they are designed to enhance the down stroke flapping motion. We have implemented this theory into a computer-aided design software called DAS-2D with a rich user-interface. It has been applied to solve several structure design problems including design optimization of compliant transmission mechanism for flapping wing MAVs, a bistable buckling beam design and a robotic finger actuated using shape memory alloy actuators.

The accomplishments and new findings of this project are listed in below:

1. We have conducted a comprehensive survey of existing MAVs from around the world. In particular, we have categorized about 15 MAVs based on workspace, compliant or rigid body, type synthesis, mobility, and actuator type. This survey is expected to serve as a resource for continued design and development of smaller and more efficient MAVs.
2. We have built a comprehensive dynamic mathematical model of the entire drive mechanism. To this end, Theodoresens theory for predicting the lifting force on an oscillating airfoil was chosen to calculate the lift force on the wing. A sensitivity analysis was performed on the model to study the effect of system variables on the performance parameters: lift produced, power consumed and lift/power ratio. The critical parameters were identified and run through an optimization algorithm to explore the design space for improving the performance of the MAV. It was seen that the power consumption was reduced by 73.8% without affecting the lift significantly. The results also suggest that some parameters affect lift and power differently, and in general, the variables do not compete with each other during the optimization. The methodology presented in the paper could serve as a tool to guide the design process during future MAV projects.
3. We verified the inclusion of compliant mechanisms in the design of the flapping mechanism as a means of reducing the load on the actuator. The mechanism for the Small Bird MAV developed by the University of Maryland was the basis of this work. The motor torque was derived in terms of rigid body mechanics, and the design parameters of the compliant members were optimized to reduce the peak motor torque during a flap cycle. Under the assumption of the constant aerodynamic load on the wings, the results indicated an 89.25% and 97.1% reduction in torque for the extension spring and compliant joint mechanisms respectively.
4. We have also worked on the design of compliant mechanisms for landing gear of MAVs. We proposed a jumping mechanism concept that utilizes a compliant mechanism, allowing the kinematics and energy storage both to be included in the elastic elements. The mechanism

weight is 9.26g, and can potentially achieve a jump height of 1m with a 19.74g payload. Pseudo-rigid-body model has been created and validated by Adams simulation. Some further work could include further optimization of the parameters for further weight reduction, as a factor of safety of 4 is relatively high and compromise of the factor of safety could be made for further weight savings. Also, different pre-selected dimensions of the device could be explored for further weight saving.

5. We have developed a parameter optimization framework for determining the pseudo-rigid-body (PRB) model of cantilever beams. PRB models are commonly used in design and analysis of compliant mechanisms since they significantly reduce the number of degrees of freedom compared with the finite element approach. Also we proposed a novel concept of PRB matrix for representing topologies of all PRB models in a uniform way.
6. We developed a theoretical model for predicting the input moment required to actuating a bistable buckled beam moving from one stable to the other stable positions. A novel experimental test setup was created for experimental verification of the model. The results show that the theoretical model is able to predict the maximum necessary input moment within an error of 2.53%. This theoretical model provides a guideline to design bistable compliant mechanisms and actuators. It is also a computational tool to size the dimensions of buckled beams for actuating a specific mechanism.
7. We studied the effects of deformation on length and cross section of the beam, and try to understand these phenomena with respect to some dimensionless parameters. These effects are more pronounced for short beams of soft materials. A few PRB models listed in literature are compared against FEA results, and optimization methods are used to determine more accurate PRB models for varying beam geometry. A study of these results will guide the discussion on how the accuracy of the PRB models changes with the beam parameters. An example of a compliant mechanism which experiences significant axial loads will be used to prove the validity of these results.
8. We have developed unified kinetostatic analysis framework for planar compliant and rigid body mechanisms. The framework was written in MATLAB and is capable of kinematic and static analysis of planar mechanisms with compliant joints or links. The simulation results were compared with the Adams software to test the validity of the framework.

1 Classification and Type Synthesis of Flapping Mechanisms for MAVs

Objective: In this task, we developed an adjacency matrix based method for classification of transmission mechanisms for flapping wing micro air vehicles. This method can be used to type synthesis of flapping mechanisms for MAVs.

Methodology: The workspace of a mechanism is defined as the set of positions that a workpiece can reach. The workpiece of a MAV is the wing, and the workspace is the generated wing trajectory. The trajectory of the wing is responsible for generating sufficient lift and thrust forces for flight. The flapping drive mechanisms are classified as planar, spherical, or spatial. The components of a planar mechanism all move in parallel planes, and utilize lower-pair joints. Theoretically, the planar joint axes intersect at infinity. A spherical mechanism generates spherically concentric motion about the spherical center of the mechanism. All the joint axes must intersect at the spherical center point. Any mechanism which cannot be classified as planar or spherical is a spatial mechanism. However, planar and spherical mechanisms may be considered special cases of spatial mechanisms, due to unique geometry and the orientations of their joint axes.

Tsai [1] has systematically classified planar and spatial mechanisms by using a graph theory. Each mechanism may be represented by a graph expressed in a so called “adjacency matrix.” Murphy [2] has extended this type synthesis to compliant mechanisms by using a similar approach. In contrast to a rigid body mechanism, each link of a compliant mechanism may be classified as rigid, compliant, or ground link. The connection types in a compliant mechanism are: kinematic pair, flexural pivot, or clamped joint. A compliant mechanism may be represented by the so called “compliant mechanism matrix”.

The adjacency matrix is a $(n \times n)$ square matrix, where n denotes the number of links or segments in the mechanism. For a given mechanism, the diagonal elements of the matrix denote the segment type, and the off-diagonal elements denote the connection types between the segments. The segment types of ground, rigid body, and compliant members are represented with a -1, 0, and 1, respectively. The connection types are as follows: no connection is 0, lower kinematic pair is 1, flexural pivot is 2, clamped connection is 3, gear pair is 4, pulley pair is 5, universal joint is 6, and scotch yoke is 7. The composition of the adjacency matrix is summarized in Figure 1. The main focus of the adjacency matrix is to capture the driving mechanism of the MAV. To allow for universal comparisons between MAV transmissions, only the simplest form of the mechanism which enables flapping motion will be analyzed using type synthesis. For example Berkeley’s MFI has four equivalent linkage mechanisms to ensure stability, type synthesis of one of these mechanisms is sufficient. If the micro air vehicle had a relatively simple passive wing rotation joint it was noted and not included in the adjacency matrix. However, if the wing rotation mechanism exceed a lower kinematic pair, then a separate adjacency matrix was developed, i.e. Berkeley’s Wing Differential I.

The most popular topology in this survey is the four-bar linkage, which is used in seven of the MAV projects. It is a relatively straightforward design, which can transform either a rotational or translational input into a reciprocating flapping motion. The five-bar linkage mechanism is the second most popular with four of the MAV projects. Different control strategies have been implemented to utilize this extra DOF, which will be discussed in the next section. Two six-bar linkages have been used in the selected MAV projects. Both designs couple two different planar

Segment Type		Connection Type	
Ground	-1	None	0
Rigid Body	0	Lower Kinematic Pair	1
Compliant	1	Flexural Pivot	2
Gear	G	Clamped	3
Cable	C	Gear Pair	4
Yoke	Y	Pulley Pair	5
		Universal Joint	6
		Scotch Yoke	7

Figure 1: Definition of segment types and connection types

mechanisms to produce the desired flapping motion. In the Jumbo Bird MAV, the coupling of a crank-slider and a dyad allows symmetry and stability in the flapping motion. In contrast, the MFI transmission allows amplification of the linear actuator through the use of a slider-crank coupled to a four-bar linkage. The last linkage based system, the Lissajous MAV, is a double spherical scotch yoke mechanism, and exhibits a very cumbersome assembly process.

The Nano Hummingbird demonstrates a unique transmission, which offers advantages and disadvantages over the traditional linkage-based mechanisms. The Nano Hummingbird originally used serially coupled four-bar linkages, which transitioned from double-rocker to a crank-rocker. Through the testing of prototypes, the design exhibited mechanical wear, radial play in the bushings, decreased efficiency, and failure. The decision was made to institute a double-pulley drive, as it reduced the number of bearing surfaces, the amount of oscillating mass, and the overall weight of the transmission. Another possible solution may have been the implementation of compliant joints, which would also reduce the number of bearing surfaces and improve the efficiency.

Since the adjacency matrix was originally designated for linkage topologies, special considerations were taken for the double-pulley drive. The driving cable has a variable length and was treated as a prismatic joint. The second cable does not change length; therefore, the pulley pairs or disks were treated as if they had directly meshed together as gears. Lastly, the connection between the pulley disk and the variable length cable was approximated as a lower kinematic pair.

The adjacency matrices and the associated characteristic polynomial coefficients are provided in Table 2 and 3. Two groups of isomorphism were detected when searching for equivalent characteristic polynomials. The first isomorphism was identical four-bar linkages: DelFly I, DelFly II, New DelFly II, and the LIPCA MAV. The second group consisted of two identical five-bar mechanisms: MFI Wing Differential I and II. It is interesting to note that the HMF and FWMAV are compliant variations of the isomorphic four-bar linkages, as seen in the adjacency matrices.

Insect-like kinematics requires control over three DOF: stroke, pitching, and stroke plane deviation. Otherwise, a MAV will approximate insect-like flight through the use of additional control surfaces. Another method is to incorporate an extra joint at the root of the wing, which allows the wing to rotate passively along its long axis. Control of the pitching action of wing has been noted in Tables 2 and 3. The only design to actively control all three DOF is the Lissajous MAV. Nine out of the fifteen MAVs have a single DOF transmission, and have auxiliary mechanisms to assist in the kinematics. Five transmissions have two DOF, and utilize different control strategies.

The first strategy is to actively control the DOF, to generate the desired wing trajectory. The MFI is an example of this method, where two parallel six-bar linkage transmissions are coupled to a single wing via the wing differential. The parallel six-bars are separately actuated to control the two DOF present in the wing differential. The opposite strategy of passive control is implemented in the PARITY MAV. In the design iteration from the HMF to the PARITY, an extra revolute joint is added between the actuator and the original transmission. The idea is to allow the passive balancing of aerodynamic loading on the wings, which is similar to the concept of an automobile's differential during a turning maneuver.

Separate from the classification of MAV transmissions is the classification of actuators, and the development of a selection database [3]. Several families and sub-types have been identified and categorized by a number of characteristics which include: maximum output strain, maximum frequency, maximum energy density, efficiency, mass, volume, and many more. Some of the major classes of actuators are electromagnetic, electromechanical, fluidic, piezoelectric, smart materials, and hybrid. The selection of actuator, power source, control system, and transmission must be integrated, as there is an inherent relationship between them.

As part of the scalability of the MAV, the selection of actuator will affect the feasibility of the design. Scaling actuators from macro to micro will result in varying performance characteristics.

In some cases, where a macro actuator type is readily available, there are challenges present in the manufacture and efficiency of the micro version. In regards to the scaling up of actuators from micro to macro, the underlying physics associated with the functioning of the actuator may not be possible [4]. In this paper we will limit ourselves to the general categorization of the type of actuator as rotary and linear, and how this impacts the mechanism design. The details of actuator selection and performance are left to detailed resources.

In terms of transmission design, the rotary and linear actuators require fundamentally different intermediary mechanisms, to transform the given input motion into a reciprocating flapping motion. There are advantages and disadvantages associated with each type of mechanism. A major difference may be how adjustable the kinematics of mechanism is, as discussed in [5]. Adjustable kinematics is more attainable in mechanism with linear actuators. Additional DOF can be added to the transmission to allow the adjustment from one flight pattern to another. Rotary based mechanisms generally have a constrained output, which limits the wing trajectory to a single, fixed path.

The majority of the MAVs included in this survey require rotary input. These nine MAVs use rotary DC motors, and the remaining designs implement linear actuators. The linear actuator based transmissions are all planar, and are specifically powered by piezoelectric actuators. The advantages and disadvantages of each actuator are discussed briefly [6–8].

The DC motor is a popular choice for MAVs, as it is reliable, versatile, exhibits high efficiency, and is readily available in the market place. Gearboxes are required to reduce the motor speed to an appropriate level, which allows the desired flapping frequency to be attained. The disadvantages of DC motors include the additional weight of the gearbox, the additional weight of a controller for brushless motors, and their limited scalability.

Lift generation depends upon the wings being able to cover a large range of flapping angles. While this may be trivial for mechanisms with continuous rotary motion, linear actuators produce little strain, and thus require mechanical amplification. In this survey, all the piezoelectric (PZT) actuators are implemented with cantilever boundary conditions and amplified with some type of four-bar linkage. The main appeal of PZTs is that they exhibit high power density and high efficiency. A major disadvantage of PZTs is that they require a high activation voltage, which is currently too large and heavy to be carried on board MAVs.

Summary of Main Results We have classified fifteen mechanisms in the literature: ten planar, two spherical, and three spatial (Table 1). In general, planar mechanisms have the advantage of being easier to design, manufacture, and assemble. The major disadvantage of planar mechanisms for MAV is the ability to generate insect-like kinematics. Additional control surfaces, auxiliary mechanisms, and actuators will be required to produce a better approximation of insect-like flight. Examples of this are the DelFly I, New DelFly II, Small Bird, and Jumbo Bird MAVs, which feature planar transmissions and tail surfaces [9]. Spherical mechanisms (i.e. Lissajous MAV) are able to generate the figure-of-eight, banana-shape trajectory, which is shown in Figure 1. With this benefit may come the complication of manufacture and assembly, as all joint axes must intersect at the spherical center of the mechanism to avoid binding. While more realistic insect-flight patterns are possible, additional DOF translates directly into additional actuators and more weight. Spatial mechanisms like spherical mechanisms are able to generate the insect-like kinematics, but may offer more flexibility in terms of adjustable kinematic parameters (i.e. not limited to concentric spherical operation). An example of this is the VTOL MAV, which is able to generate four different flight patterns. When compared to the simplistic nature of planar mechanisms, the manufacture and assembly of spatial mechanisms is more challenging.

There are three types of compliant mechanisms, which will be considered during this classi-

fication: compliant or flexural joints, short compliant segments, and long compliant segments. Flexural joints localize the compliance in the mechanism, and typically allow small deflections. Flexural members distribute compliance in a mechanism to enhance the desired transformation of motion and forces. Short compliant segments exhibit relatively small deflection, when compared to the large and possibly non-linear deflections of long compliant segments.

As part of this classification, the transmissions were sorted by segment type as follows: seven rigid body mechanisms, seven compliant joint mechanisms, one short compliant member mechanism, and no long compliant member mechanisms. It is interesting to note that only planar mechanisms feature compliant components; however, the MFI wing differentials do feature compliant joints. Of the compliant mechanisms, the use of the flexural joints dominated, which may be due to their relatively easy analysis and fabrication. In Section 2.2, the advantages and disadvantages were discussed in detail.

The University of Maryland's Small Bird MAV demonstrates the ideal application of compliant mechanisms. The Small Bird uses flexural members to reduce the peak motor torque. The motor experiences peak torque at the beginning of the up-stroke and the down-stroke, due to the aerodynamic loading of the wings. When the crank and coupler reach over-center, the compliant frame reaches its maximum deflection. Once the crank pulls away from the maximum point, the compliant members release their stored energy, and assist the motor in overcoming the peak aerodynamic loading in the stroke cycle. The compliant frame was manufactured as a single piece, using injection molding. This reduces the use of traditional joints, decreases the weight of the transmission, decreases the part count, and improves the overall efficiency of the transmission. For a larger size MAVs, such as the Jumbo Bird, flexural joints were used to avoid long compliant segments, which may behave non-linearly and negatively affect the stability of the MAV.

The importance of this classification lies in that it lays out the foundation of type synthesis of flapping wing mechanisms. Type synthesis is the process of defining the type a mechanism, which is best suited for a given problem. The input to the type synthesis process include (1) type of input motion (translational or rotational), (2) flapping frequency of the output beating motion, (3) desired mobility (number of actuators) and (4) choice of planar or spherical or spatial solutions. This is typically a creative stage in a design process.

2 Optimization of Mechanism Design for a Flapping-Wing Micro-Air-Vehicles

Objective : Development of design guidelines regarding the effect of different parameters of flapping wing MAVs on lift production and power consumption. Optimization of these variables using modeling and simulation will improve the performance based on the project goals.

Methodology: Development of flapping wing MAVs currently follows an ad hoc approach, where successive designs are tested until one is obtained that satisfies performance requirements. For example, during the development of the Nanohummingbird [26], the team at AeroVironment tried more than 50 different wing shapes and structures. A quantitative approach may be developed which can be undergo an optimization process so as to yield better performance in the form of increased lift, reduced power consumption or other key objectives.

Three key performance characteristics for an MAV are power consumption, maximum payload the vehicle can carry, and the lift to power ratio (sometimes replaced by the thrust to power ratio). The important parameters that affect these performance characteristics are the motor characteristics, the shape and size of the wing and the mechanism kinematics. For the mechanism performance, the important variables are the dimensions of the linkages. The mechanism being considered also has compliant elements, which leads to the definition of spring constants and equilibrium positions. By optimizing these parameters, we can expect an improvement in the performance of the MAV.

Table 1: Classification of Flapping Mechanisms

Research Group	Project	Workspace Type	Topology	Rigid Body or Compliant	Actuator Type	Transmission Mobility	Wing Rotation	Year Ref.
AeroVironment	Nano Hummingbird	Planar	Double Pulley Drive	Rigid Body	DC Motor	1	Active	2012 [10]
Berkeley	MFI Transmission	Planar	6-bar	Compliant Joints	PZT BiMorph	1	N/A	2007 [11]
	Wing Differential I	Spatial	5-bar	Compliant Joints	N/A	2	Active	2002 [12]
	Wing Differential II	Spherical	5-bar	Compliant Joints	N/A	2	Active	2003 [13]
Warsaw/Cranfield University	Lissajous MAV	Spherical	Double Scotch Yoke	Rigid Body	DC Motor	3	Active	2005 [14]
DRDO (India)	VTOL MAV	Spatial	4-bar	Rigid Body	DC Motor	1	Active	2009 [15]
Delft University	DelFly I	Planar	4-bar	Rigid Body	DC Motor	1	Passive	2009 [16]
	DelFly II & DelFly Micro	Spatial	4-bar	Rigid Body	DC Motor	2	Passive	2009 [17]
	New DelFly II	Planar	4-bar	Rigid Body	DC Motor	1	Passive	2010 [18]
Harvard	HMF	Planar	4-bar	Compliant Joints	PZT BiMorph	1	Passive	2008 [19]
	PARiTy	Planar	4-bar	Compliant Joints	PZT BiMorph	2	Passive	2010 [20, 21]
Konkuk University	LIPCA MAV	Planar	4-bar	Rigid Body	LIPCA	1	Passive	2008 [22]
University of Delaware	FWMAV	Planar	4-bar	Compliant Joints	DC Motor	1	Passive	2005 [23]
University of Maryland	Small Bird	Planar	5-bar	Short Compliant Segments	DC Motor	2	None	2010 [24]
	Jumbo Bird	Planar	6-bar	Compliant Joints	DC Motor	1	None	2009 [25]

Compliant mechanisms are used in the design since they reduce problems with assembly and eliminate wear and tear due to relative motion and the need for lubrication [27], and can also reduce power consumption. The base mechanism chosen for the design process is the Jumbobird [25] developed by University of Maryland.

The aerodynamic forces on the wing were calculated using equations developed by Theodoresen for the forces and moments that act on an airfoil with an aileron which is undergoing flapping motion in a stream of fluid of constant velocity [28]. The lift equation for the wing is given by

$$L = \rho b^2 (\pi \ddot{h} + v \pi \dot{\alpha} - \pi b \alpha \ddot{\alpha}) + 2 \pi \rho v b C(k) Q \quad (1)$$

where ρ is the density of air, b is half the chord length and v is the forward velocity of the wing. $C(k)$ and Q are defined in Ref. [28].

The main focus of this work was to develop a dynamic model of the flapping mechanism of an MAV so that the effects of different parameters on the performance of the MAV can be easily studied. The mechanism is shown in Fig. 3. A modular approach was used in the development of

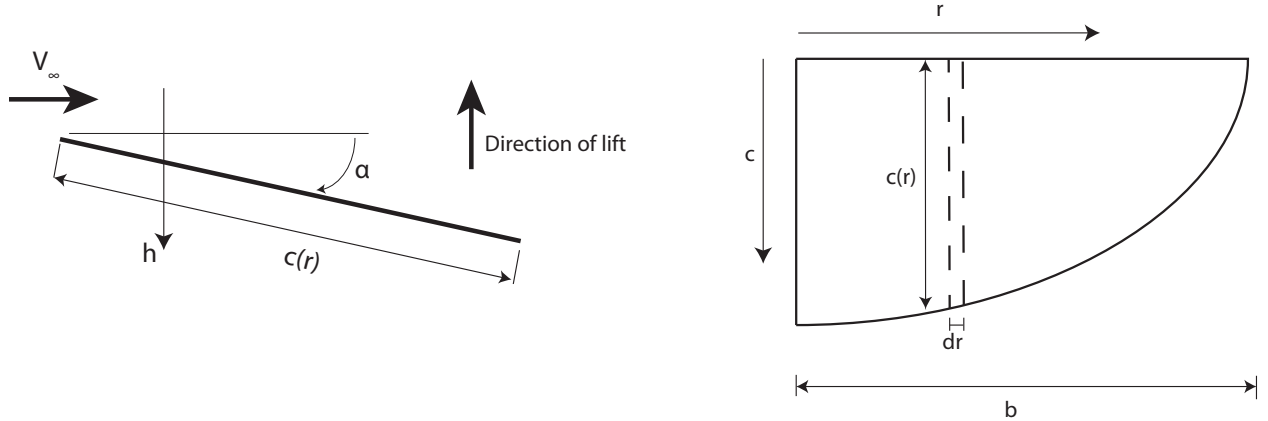


Figure 2: Section of spanwise blade element of wing and planform of wing

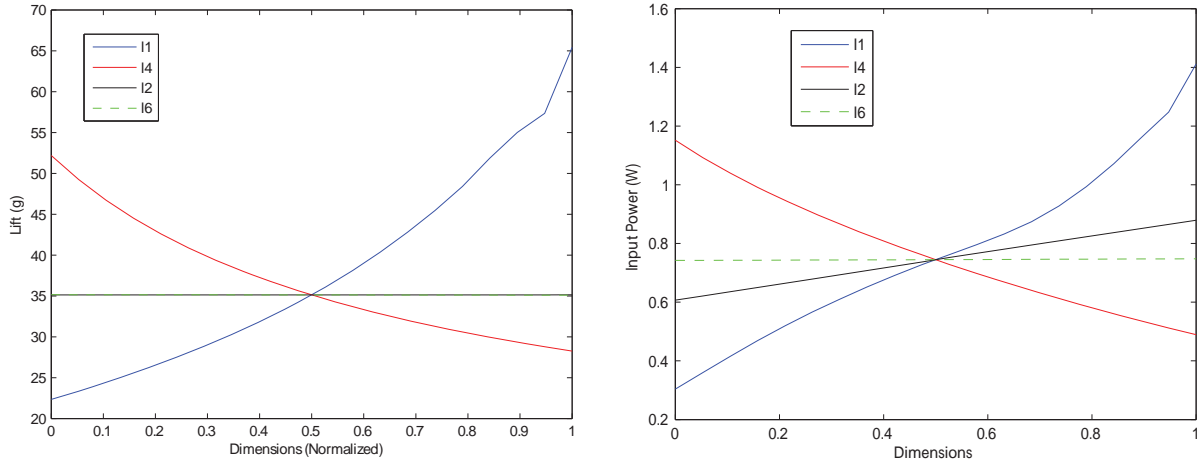


Figure 4: Variation of lift and power with kinematic parameters

the model so that improvements could be made to the aerodynamic force, the motor model, the compliant mechanism theory and the optimization without affecting other parts of the code. The masses and moments of inertia of the rigid links were estimated using the mechanism dimensions. The values of the spring constants were calculated using the pseudo rigid body model.

The MAV, being a complex system, has a large number of parameters that can be varied, which means that the design space would extend into a large number of dimension. Since our goal is the optimum design of the MAV mechanism, we looked at the how different system parameters affect the performance of the system. With this data, we could try to identify the crucial variables and work on optimizing only these parameters which would significantly reduce the load on the optimization algorithm. The design variables were divided into two: (1) kinematic parameters and (2) system parameters.

The kinematic parameters mainly refer to the lengths of the different links, and these affect the kinematics of the mechanism. Fig. 4 shows the variation of lift and power when each of the link lengths was varied while keeping the other values constant. It was observed that links 1 and 4 affected lift production and power consumption significantly, whereas link 2 affected only power consumption.

The system parameters refer to other variables in the system, such as wing size, motor characteristics and joint stiffness. The important system parameters which were incorporated in the model were identified as angle of attack of the wing, the average flapping frequency, the forward velocity of the MAV, and the wing size which was determined by mean chord length and wingspan. Fig. 5 is a graph showing mean lift produced with variation in different parameters while keeping

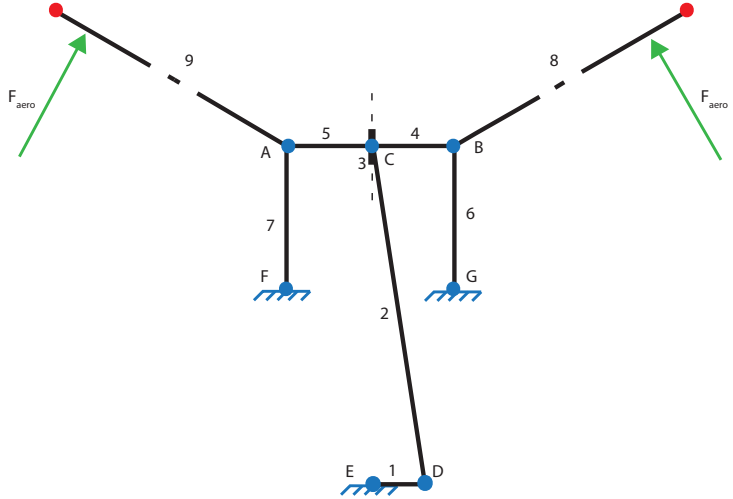


Figure 3: Schematic of flapping mechanism

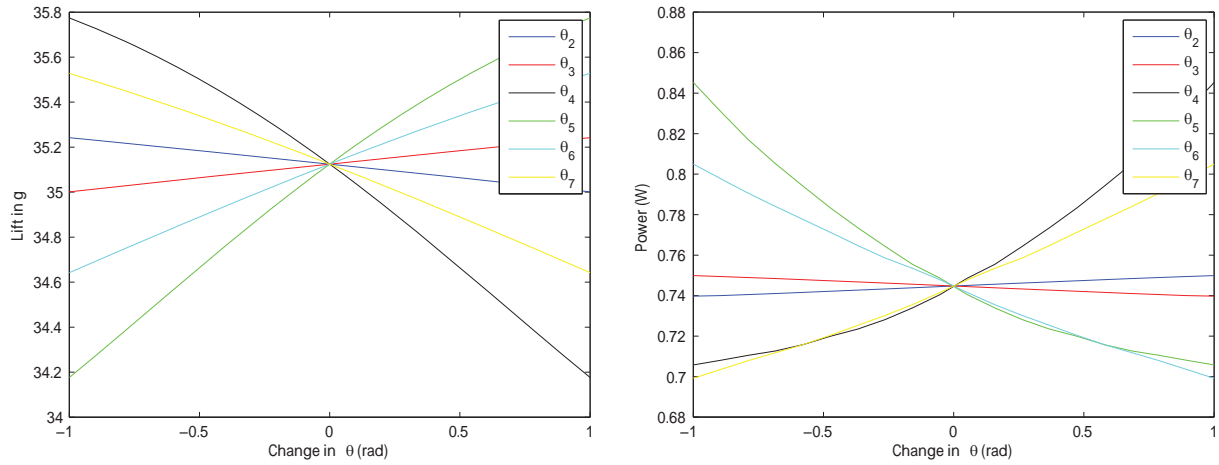


Figure 6: Variation of lift and power with equilibrium position of springs

the other values a constant. Since the mechanism has a few compliant joints, there exists the possibility of using the parameters of the compliant elements to achieve the required system performance. As explained earlier, the compliant joints were modeled as torsion springs, and therefore, it would be possible to vary the equilibrium positions of the springs. In reality, this can be achieved by changes in the fabrication process, such that the spring compliant elements are in a prestressed state when assembled. Fig. 6 describes the effect of varying these equilibrium angles on lift and power. The variation in lift is not very high, whereas power varies significantly. It is clearly beneficial to assemble the mechanism such that certain springs are always in a state of compression or expansion.

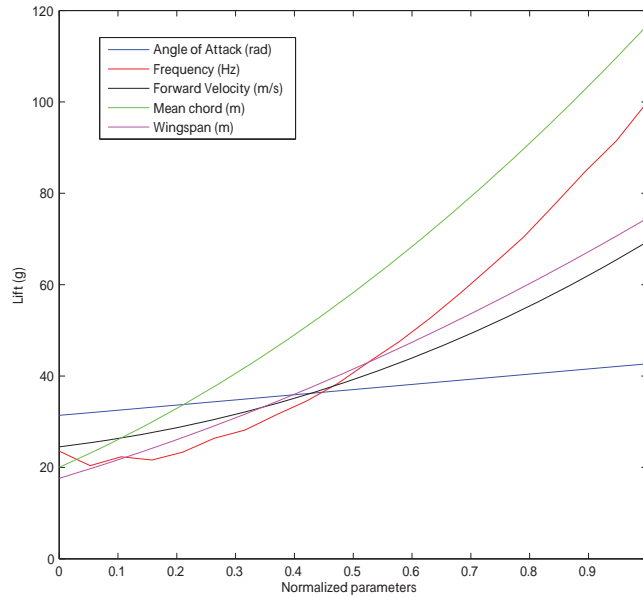


Figure 5: Variation of lift with system parameters

A series of optimization runs was conducted to achieve the best design where the variables which had the largest influence on performance were optimized. A range of values was provided for each of the variables keeping in mind the size of the system and other practical constraints. Due to factors pertaining to the accuracy and robustness of the aerodynamic model, care was taken to ensure that the flight regime of the MAV did not change drastically. The aim of the optimization was either 1) to produce maximum lift without consuming more power, or 2) to minimize the power consumption without reducing the lift produced.

The variables used in the optimization were dimensions of two of the mechanism links, l_1 and l_4 , the angle of attack of the wing, α , the width of the compliant joints, w , and the initial configuration of the joints, defined by $\Delta\theta_G$. The results of the optimization are shown in Table 4.

Fig. 7 shows the change in lift produced from optimization for maximum lift. In this case, the

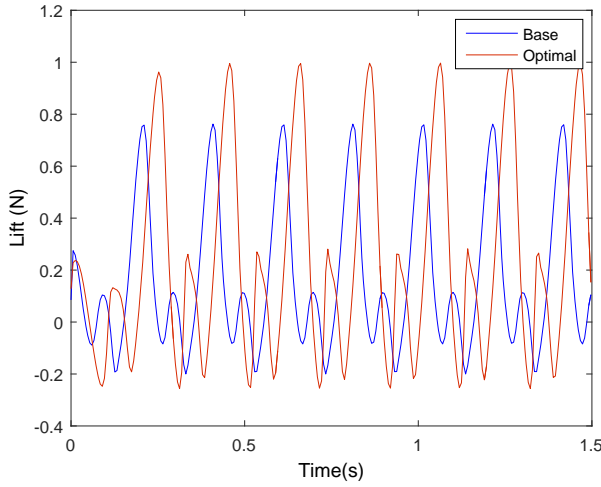


Figure 7: Comparison of lift produced during flapping motion before and after optimization for maximizing lift

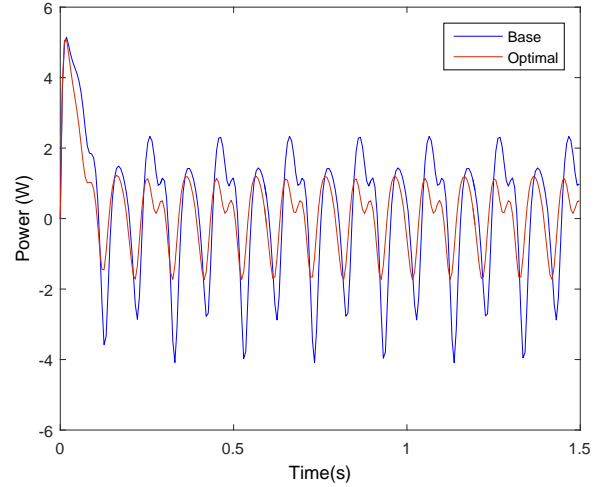


Figure 8: Comparison of power consumed during flapping motion before and after optimization for minimizing power

mean power consumption is not allowed to exceed the base value of 0.745W. The graph clearly demonstrates the increase in lift with higher and wider red peaks compared to blue peaks. Fig. 8 shows the possible reduction in power consumption when 35g of lift is required. Since the negative power values are ignored, it is seen that the positive peaks are smaller than before optimization, and should result in lower power consumption.

Close inspection of Table 4 suggests that increasing the constraint on power consumption does not provide a substantial increase in lift produced. For example, changing the maximum power consumption from 0.745W to 0.9 W only increases lift from 48.95g to 54.72g. However, reducing the mass of the system, that is, the minimum lift required from 35.12g to 30g reduces the power consumption from 0.4044W to 0.2151W. This means that it is more beneficial to focus on reducing the mass of the system compared to using a more powerful motor. It was also noticed during the optimization that it is beneficial to have the springs in the system in such a configuration that they aid the downward motion of the wing (during which the lift is produced). The optimization moves towards the region where the equilibrium position of the springs is at the bottom of the flapping motion.

Summary of Main Results : The dynamic model is a useful tool to study the performance of the system with respect to different design parameters. The sensitivity study provides valuable insight into contribution of individual parameters towards the generation of lift as well as power consumption. Once these parameters are identified, the design can be optimized for required performance goals.

A salient feature of a majority of the results was that the optimal values were usually at the upper or lower bounds of the variables, which means that improvements in the performance of the MAV appear to be limited only by fabrication and size constraints. However, some of the assumptions involved in the development of the model must be kept in mind while attempting to change the parameters. One of the significant limitations is the reliability of the aerodynamic model in accurately predicting the forces on the wing.

Depending on the compliant joint, the pseudo-rigid-body model can be altered for more accurate results. Some accuracy issues can be overcome by developing a better system model, which may require higher computing ability. The aerodynamic model itself can be improved by incorporating

all the dominant aerodynamic effects. Considering how complex such a force model would be if derived from basic principles, a heuristic or surrogate model would be much more compatible.

A summary of the design guidelines is given below.

1. If compliant joints are present, they should be assembled such that the stiffness aids the downward motion of the wing. This can also be achieved by using regular springs.
2. The focus of the design process should be on reducing the mass of the system rather than increasing the power available to it.
3. Increasing the flap angle leads to simultaneous increase in lift production and power consumption. For the system described here, the increase in power is greater than the increase in lift.

The approach described provides a set of guidelines for design of a flapping wing MAV for suitable dynamic performance. This method can be altered to fit the application in question, but they are general principles that can be used for any dynamic compliant mechanism. With the choice of a suitable aerodynamic model, the external forces on the system can be determined with minimal computation. A simple dynamic model can be used to approximate the performance of the system, and the sensitivity study determines the important design parameters. Using this information, an optimization algorithm can be utilized to arrive at the mechanism design that leads to optimal performance.

3 A 3-spring Pseudo Rigid Body Model for Soft Joints with Significant Extension Effects

Objective: The goal is to derive a rigid body approximation that can capture the extension effects in similar compliant joints. We have derived a 3-spring revolute-prismatic-revolute pseudo-rigid-body model for short beams used in soft joints made of elastomer material. These elastomer joints are often used in compliant transmission mechanisms for flapping wing MAVs.

Methodology: Compliant mechanisms are those in which conventional rigid-body elements such as pin joints are replaced by deformable members or flexures. Methods for analysis and design of compliant mechanisms have improved significantly over the last couple of decades. This work deals with a technique that uses the pseudo rigid body (PRB) model, most of the groundwork for which was laid down by Howell and Midha [29,30]. Since the behavior of deformable members is difficult to introduce into the kinematic study of a mechanism, they are converted to rigid body links for the ease of analysis. For instance, a flexure pivot may be replaced by a revolute joint and a torsion spring.

Many PRB models have been developed, each more accurate than the previous one, but with accuracy comes the cost of complexity. For beam type compliant elements, Dado [31] developed a variable parametric model and Su [32] came up with a model with 3 revolute joints. However, most PRB models only account for the transverse deformation of the beams, while the axial deformation of the beams is ignored. In this work, the model presented will also take axial deformation into consideration. Vogtmann et al. [33] developed a similar model for elastomeric joints to account for extension and torsion effects, demonstrating the need to include extension springs for soft joints. It provided a quick derivation of the PRB parameters, and was shown to be accurate for specific types of joints. The approach in this paper is more general and detailed, and introduces a rigid segment at either end of the beam which is shown to affect the error in the model.

The PRB model has to be compared with an analytical or an FEA or a physical model to determine the values of the parameters. For this case, a beam model approximation based on

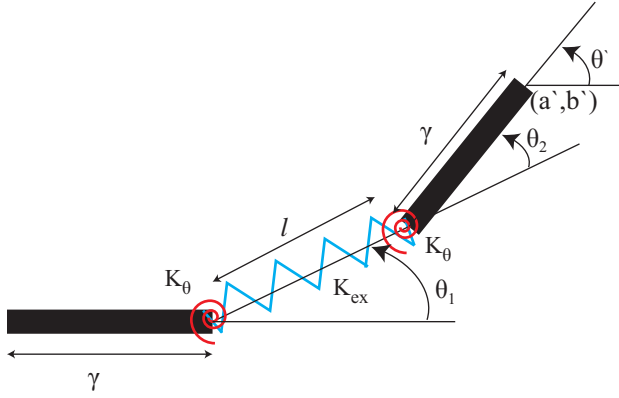


Figure 10: The 3-spring PRB model after deformation

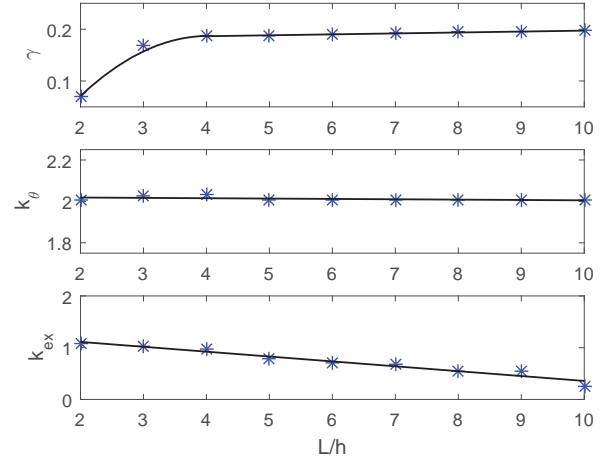


Figure 11: Optimal PRB parameters for RPR model as functions of length to height ratio

Timoshenko beam theory [34, 35] has been developed. The model is analyzed over a large range of general loads and a comparison is made between the Timoshenko beam model and PRB model. An optimization process is carried out to determine the PRB model parameters that give the least error. Figure 9 shows a few soft joints using the SDM technique at the Design, Innovation and Simulation Lab (DISL). The flexible parts are made from a rubber-like material of very low modulus of elasticity. During testing, it was seen that due to the low elastic modulus of the material, the flexures also undergo axial deformation and Poisson's effect. A beam model was developed that takes these effects into account and used it to derive a pseudo-rigid-body model for computational purposes.

In order to account for the various behavioral characteristics of the soft joint, a pseudo-rigid-body model of three segments was developed. The model is a revolute-prismatic-revolute (RPR) serial chain. A schematic of the same is shown in Fig. 10. The schematic is for a beam of unit length. The base model is symmetric, i.e. the parameters are the same at either end. There are two rigid beams of length γ . An extension spring of stiffness K_{ex} is attached to both the rigid members through revolute joints. Torsion springs are present at both the revolute joints, of spring constant K_{θ} . The extension spring is not capable of bending, as if a prismatic joint is present between the two revolute joints. The torsion springs account for the bending stiffness of the beam, and the extension spring represents the axial stiffness. The undeflected length of the extension spring is l_0 .

A modified Timoshenko beam approximation was used to determine the deflection of the beam under the action of tip loads, including bending, shear, extension and Poisson's effect. The results

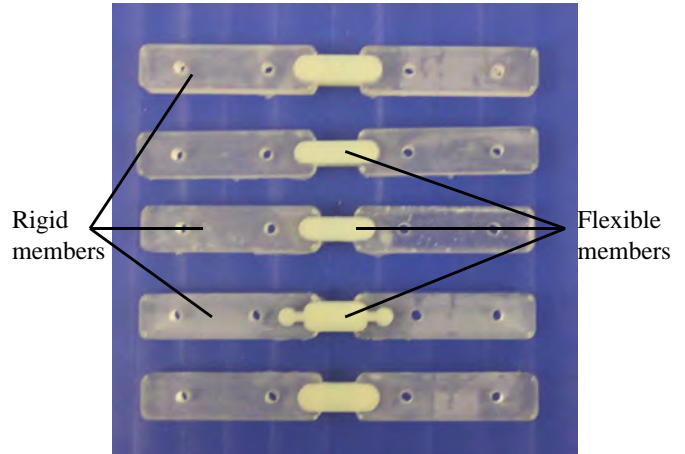


Figure 9: Joints fabricated using shape deposition manufacturing at Design, Innovation and Simulation Lab at OSU.

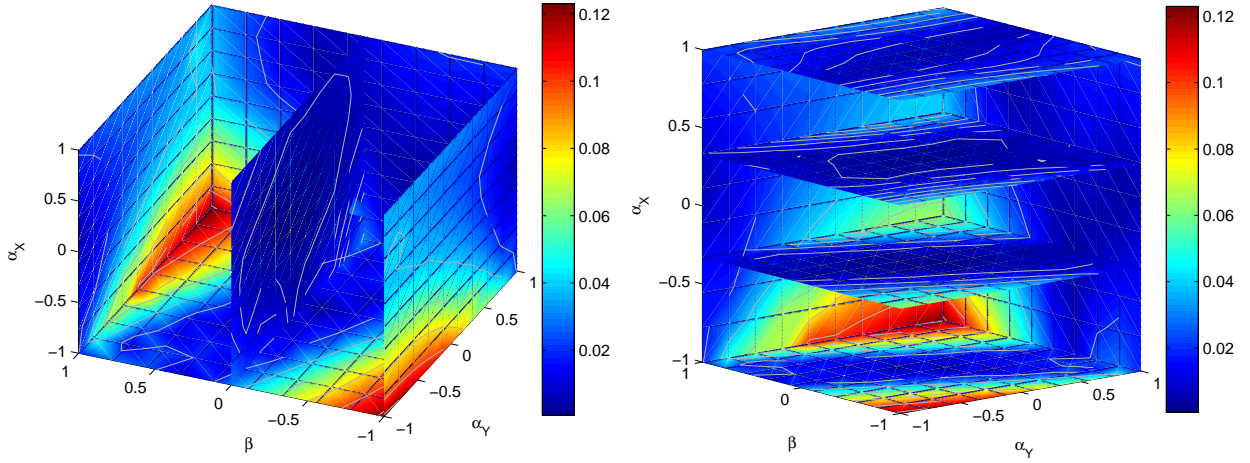


Figure 12: Variation of error in PRB model with loads (for the joint with $L/h = 2$). α_x and α_y are tip forces in the axial and transverse directions. β is the bending moment at the beam tip.

from this method were used to calculate the optimal values of the PRB parameters over a range of loads.

The extension effects in the soft joints are expected to change with respect to the ratio of length to width for the compliant joint. Nine values of the length to height ratio (for beams of rectangular cross-section) were considered, with the L/h ratio varying between 2 and 10. The optimal values of the PRB parameters obtained for each case are shown in Fig. 11, with the curve fitting functions given below.

$$\gamma = \begin{cases} -0.0281 \frac{L^2}{h^2} + 0.2266 \frac{L}{h} - 0.2698 & ; \quad 2 \leq \frac{L}{h} \leq 4 \\ 0.0018 \frac{L}{h} + 0.1792 & ; \quad 4 \leq \frac{L}{h} \leq 10 \end{cases}$$

$$k_\theta = -0.0017 \frac{L}{h} + 2.0220$$

$$k_{ex} = -0.0942 \frac{L}{h} + 1.3002$$

Figure 12 shows the details on the variation of error with the loads viewed as contour slice plots. A thorough reading of the plots indicates that the error is very low (below 0.02) for a large range of loads, and the only regions of high error are when all the loads work towards deflecting the beam in the same direction, i.e. $\alpha_x = -1$ and $\alpha_y = \beta = \pm 1$. The error plots clearly indicate that errors creep into the model only for very large loads, and it works extremely well for tip deflections as high as 70° . A sensitivity analysis was also performed near the optimal point to determine the significance of each PRB parameter on the error. The results of the study for the shortest beam ($L/h = 2$) are presented in Fig. 13. A reading of the vertical axis of the graphs also indicates that the change in error due to k_{ex} is much less than the change in error due to either k_θ or γ . Thus, the results are more sensitive to changes in the latter two parameters.

Summary of Main Results: The pseudo-rigid-body model approximation described in the form of a revolute-prismatic-revolute (RPR) member is capable of representing the bending and extension stiffness of the compliant soft joint. Due to the combination of bending and extension effects, the PRB parameters are dependent on the aspect ratio of the beam, but still independent of the modulus of elasticity and can be used for different dimension scales.

The PRB model presented here is limited by the effectiveness of the beam theory used to

calculate the force-deflection relationship. With a better understanding of the material behavior and better solution techniques, it is possible to improve the characteristics of the model. Currently, it is limited to the linear elastic regime of the material. The deformation of the members is also restricted to bending and extension, without considering distortion of the cross-section.

The integration of extension effects into the analysis of compliant members and the PRB model, the optimization approach and the fitting functions of the PRB parameters are the main contributions of this work. The simplicity of the PRB models when compared to beam models or FEA makes them ideal candidates for design and analysis of compliant mechanisms, for computational reasons or when using an intuitive design approach. By reducing the error and developing a general framework, it is possible to create a design approach for compliant mechanisms using PRB models.

4 A Parameter Optimization Framework for Determining the Pseudo-Rigid-Body Model of Cantilever Beams

Objective : Development of a framework for determining the optimal pseudo-rigid-body (PRB) model of 2D cantilever beams. This method can be used for deriving numerical approximations for compliant elements for various applications.

Methodology: The design of compliant mechanisms can be a difficult process due to the nonlinearities arising out of their deflections. This places a great emphasis on the need to improve the methods of analysis. With a better understanding of behavior of compliant elements and enhancing the tools for analysis, there will be a significant advancement in the use of these mechanisms. The approach used in this work replaces flexible elements with pseudo-rigid-body (PRB) models, which simplifies the statics and kinematics equations. Since rigid-body kinematics are well studied, the PRB approach is usually more intuitive for the purpose of analysis and design. However, care needs to be taken to ensure that the model is accurate in replicating the behavior of the flexible members.

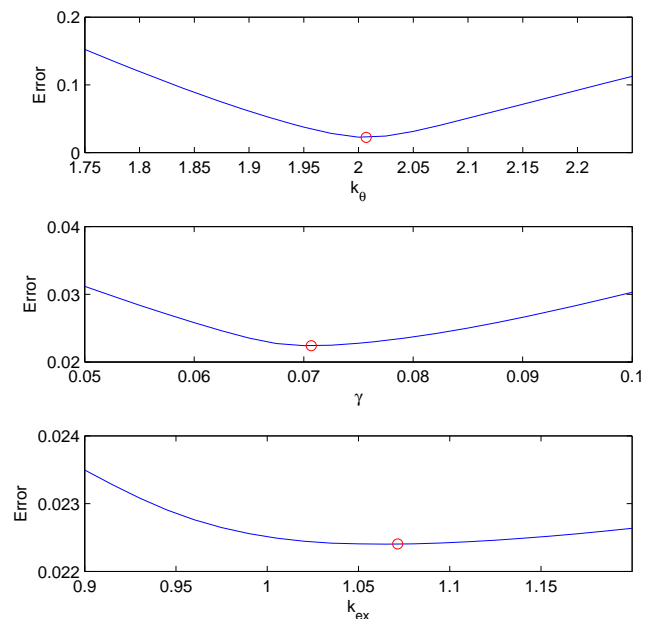
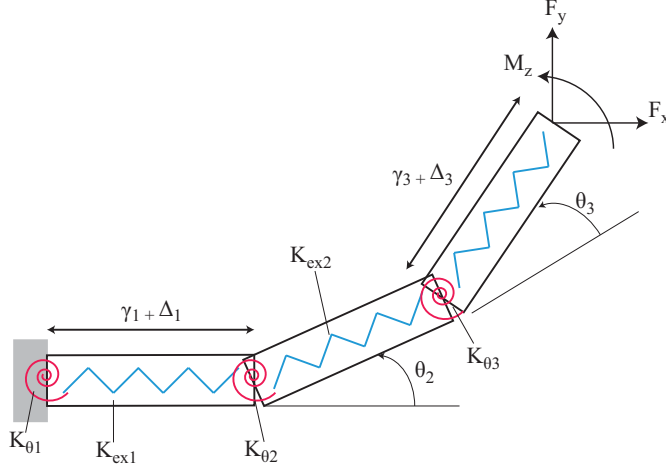


Figure 13: Sensitivity of individual PRB parameters near the optimal point for RPR model

Apart from the articles mentioned in Sec. 3, multiple research groups have focused on PRB models over the past decade or so. Chen et al. [36] used a particle swarm optimizer to suggest better values for the parameters of the 3R model derived by Su [32]. But this model may be too complex for simple elements, leading to increased computational cost. Recently, Yu et al. [37] proposed a 2R model that reduces the complexity of the 3R PRB model while maintaining a similar level of accuracy. Another method for using PRB models with revolute joints was suggested by Pei et al. [38]. Some models also use prismatic joints with extension springs, such as the one presented by Saxena and Kramer [39] or Vogtman et al [40].

One of the major drawbacks of most of these models is the dependence of the parameters on the loading direction. Although this is useful for static analysis, where the loads and boundary conditions are known, it makes these models difficult to use for dynamic simulations or mechanism



$$\Omega = \begin{bmatrix} k_{\theta 1} & k_{ex1} & \gamma_1 \\ k_{\theta 2} & k_{ex1} & \gamma_2 \\ k_{\theta 3} & k_{ex1} & \gamma_3 \end{bmatrix}$$

$$K_{\theta i} = k_{\theta i} \frac{EI}{L} \quad ; \quad K_{exi} = k_{exi} \frac{EA}{L}$$

Figure 14: General PRB model with 3 elements with its PRB matrix

synthesis. Load independent models are more useful for these cases. Since compliant mechanisms usually have a limited range of motion, the models only have to be accurate within the expected range of loading or deformation. It may also be important to have model parameters based on the type of deformation expected.

The required accuracy and kinematics of the PRB model also depend on the application. It may be useful to develop a model on a case to case basis after studying expected deformation, required accuracy and other application requirements. With this in mind, a strong argument can be made for a general PRB model that can be adapted for each case. The model can be altered to be simple or complex based on the demands of the application. Since the design process generally involves multiple evaluations, a simple model with minimum parameters would be suitable for this. For analysis, the user may be better served having a complex model that captures all the characteristic behavior of the compliant element.

Pseudo-rigid-body models serve as replacements for compliant elements. This means that they should have properties similar to those of the original elements they replace. Compliant members can undergo deformation, but also provide a resistance to deformation due to the intrinsic material properties. In order to capture these properties, most PRB models consist of joints, which define the degree of freedom, and springs, which represent the stiffness of the material. If the fundamental elements that can represent these characteristics are identified, it is possible to develop any PRB model as a combination of these elements. This is the basic idea behind the general PRB model.

Since most of the PRB models currently in literature only involve revolute joints with torsion springs and prismatic joints with extension springs [41], the scope of this discussion will be limited to similar segments. In theory, it is possible to add any segment that is representative of any kind of deformation or stiffness. Additionally, only springs with constant stiffness will be considered, although nonlinear stiffness functions can also be expressed using this method. Figure 14 shows a schematic diagram of a general PRB model with 3 elements.

One important aspect of the general PRB model is the number of parameters needed to define it. In the basic form discussed in this paper, each segment has 3 parameters, which translates to 9 parameters for a model with 3 segments. A convenient method of representation is necessary for these parameters. To this end, a simple tool which called the PRB matrix was defined. This matrix consists of the values of the different parameters, with the number of rows equal to the number of segments in the model. Each row contains the values of k_{θ} , k_{ex} and γ for each segment. The symbol Ω is used to represent the PRB matrix. A representation of a 3x3 PRB matrix is shown on

the right side of Fig.14.

The estimation of PRB parameters can be done using a variety of methods. Most of the early work on PRB models focused on understanding the behavior of the beam, and deriving the PRB model and the values of the parameters based on observed results [42,43]. While this works very well on a case to case basis, it is very difficult to use in an algorithm to find the most optimal PRB model. A few new papers have talked about using different mathematical techniques for arriving at the optimal PRB parameter values [36]. An effective method is to perform a straightforward optimization on the parameters with the objective of trying to minimize the error in the model compared to results from established methods such as beam theory, FEA or experiments. In this work, the optimal PRB parameters were calculated using a local optimization routine to minimize the error between the PRB model and the beam theory results over a large number of loading cases.

Tables 5, 6 and 7 show various possible topologies of the PRB model using combinations of the three basic types of segments. The tables also list the degrees of freedom of the model and the number of independent PRB parameters. The error value represents the mean error over the range of loads for the optimized version of each model. The optimal values of the parameters are also listed. In cases when similar PRB models have already been listed in literature, the reference number has been provided next to the name.

It is possible to use a simple algorithm to choose the best PRB model for a given application. First, the deflection of the relevant compliant member must be determined using beam theory, FEA or experiments for various loading cases. An error calculation function must be developed to determine the error over all loading cases for any given PRB matrix. Using tables 5, 6 and 7 as guides, an optimization algorithm can be used to run through various PRB models to find the most optimal one for the application.

Summary of Main Results: The definition of the PRB matrix, which allows the uniform representation of many pseudo-rigid-body models, is an important contribution. It can be used to represent varying topologies of PRB models and also the different elements in them. The development of the optimization framework, which facilitates the user to find the best PRB model with optimal parameters for a given application, is the most important contribution. In this work, a direct optimization method has been used to calculate the optimal values in the PRB matrix. The definition of the error function is subjective, and may be changed depending on the application.

The general PRB model could serve to be a useful tool in the analysis, and possibly synthesis of compliant mechanisms especially in the early design stages. It eliminates the need to determine the best PRB model by an ad hoc approach. Moreover, this procedure can be easily extended to a variety of compliant elements. Also the PRB matrix will be implemented into a computational design software for compliant mechanisms currently being developed at The Ohio State University.

5 DAS-2D: A Concept Design Tool for Planar Compliant Mechanisms

Objective: Currently design and analysis of compliant mechanisms rely on several commercial dynamics and finite element simulation tools. However these tools do not implement the most recently developed theories in compliant mechanism research. In this task, we present Compliant DAS-2D (**D**esign, **A**nalysis and **S**ynthesis), a conceptual design tool which integrates the recently developed pseudo-rigid-body models and kinetostatic analysis/synthesis theories for compliant mechanisms.

Methodology: In terms of computer-aided design of mechanisms, there has been a number of static solvers that have been developed throughout the years and KINMAC (KINematics of MACHinary) and STATMAC (STATics of MACHinary) by Paul [44] are maybe the first examples of the kinematic and static analysis tools. SAM [45] is a commercial software capable of kinematic

and static analysis limited to rigid-body linkages. More recently CoMeT [46] [47] was developed for static analysis of compliant mechanisms which is not limited to just the planar cases. However direct stiffness method was employed in the software which is only accurate for small deflections of elastic members limiting the capabilities of the software. Geometrically Exact Beam Theory (GEBT) [48] is a FEM tool for static analysis of structures but it is not possible to analyze mechanisms that contain moving joints. Similarly, SPACAR [49] is a software package for dynamic modeling and analysis of multibody flexible systems with finite element analysis. WorkingModel 2D is a commercial software for multi-body dynamic simulation of planar physical systems. It has been often used in design and simulation of planar mechanisms. Matlab's SimMechanics toolbox is a powerful multi-body dynamics solver however the design process with block diagrams is not entirely intuitive and the toolbox lacks of proper interactivity between the user and the simulation. Yue et al. [50] have developed virtual reality user interfaces that communicate with SimMechanics solver for interactive design of planar mechanisms. Adams [51] is a commercial software capable of dynamic simulation of planar mechanisms.

Given numerous advances in compliant mechanism theories in the past two decades, they have not been implemented into any design software that is dedicated to design of compliant mechanisms. Here we aim to fill this gap by developing a conceptual design software that integrates kinetostatic analysis and synthesis theory for design of compliant mechanisms. Kinematics of rigid-body mechanisms will also be a side product of this software since they are considered as special subset of compliant mechanisms. The software was developed with the graphic user interface in MATLAB to take advantage of the built-in functions of nonlinear equation solvers and optimization routines.

It is well known that analysis of compliant mechanisms involves simultaneously solving a set of kinematic equations coupled with static force equilibrium equations, which are called kinetostatic (kinematic and static) equations. Complex number method is one of the most commonly used method in kinematic analysis:

$$\vec{Z} = re^{i\theta} = r(\cos \theta + i \sin \theta) \quad (2)$$

where $i = \sqrt{-1}$ is the complex number unit. In general, the vector loop equation for a mechanism with l independent closed loops can be written in the complex form:

$$\sum_{i=1}^n C_{ki} \vec{Z}_i = 0, \quad 1 \leq k \leq l \quad (3)$$

where coefficient C_{ki} can be -1, 0 or 1.

Graph theory is often employed in representing mechanisms [52–54]. This representation is widely used in classification and type synthesis of rigid-body mechanisms. The two different graphical representations of the same slider-crank mechanism are showed in Fig. 15. At the top, Freudenstein and Maki [55] give an example of the common practice in which vertices represent links and the edges for kinematic joints. Since rigidly connected vertices are represented with a single vertex, this representation is not well suited for implementation. Also only binary joints can be handled with this representation without breaking multiple joints into binary joints. Therefore a new representation is adapted over the traditional method. In this new representation, vertices represent the nodes (or the joints) and the edges denote the links between the joints. This new representation is parallel with how individual links are stored in the software.

The main challenge of kinematic analysis is finding independent loops for formulating kinematic constraint equations. In the graph theory, the topology of any mechanisms is represented in the adjacency matrix. And the number of independent kinematic loops can be calculated with the Euler's formula. Once the adjacency matrix and the number of independent kinematic loops are determined, graph theory can be used to find the cycle bases (independent loops).

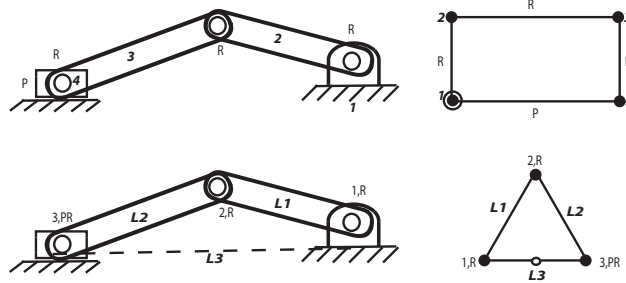


Figure 15: A slider-crank mechanism its the graph theory representations: the classical graph representation (top) and the new graphical representation implemented in Compliant DAS-2D.

After all independent kinematic loops are found, nonlinear kinematic equations of the mechanism can be readily derived as the following. The kinematic equation for the i th link can be written as:

$$\vec{Z}_i = \vec{Z}_{i0} + \lambda_i \times \vec{f}_i(x_i), \quad (4)$$

where \vec{Z}_{i0} and λ_i are constant design parameters for the link and \vec{f} is a function for which input is the unknown parameter(s) needed to define the link. As an example, for a binary link with two pin joints, the term \vec{Z}_{i0} is zero, $\lambda_i = r_i$ is length of the link. And $\vec{f} = (\cos \theta_i, \sin \theta_i)^T$ where θ_i is the link angle.

Following this notation, for a mechanism with n links and l independent loops, the kinematic constraint equations can be systematically derived as n vector equations or $2n$ scalar equations:

$$\sum_{i=1}^n C_{ki} \vec{Z}_i = \begin{Bmatrix} 0 \\ 0 \end{Bmatrix}, \quad 1 \leq k \leq l \quad (5)$$

where coefficient C_{ki} can be -1, 0 or 1.

By applying Eq.(5), kinematic equations will be formed and they can be solved simultaneously using a nonlinear equation solver with the number of inputs equal or less then the degrees of freedom of the mechanism.

Compliant mechanisms have at least one compliant link that can be deformed under external forces. PRB models have been widely used in the analysis and synthesis of compliant mechanisms. In this approach, n rigid segments are joined with torsion and or extension springs. Fig. 16 shows example PRB model of a cantilever beam. Several PRB models were developed to analyze elastic members.

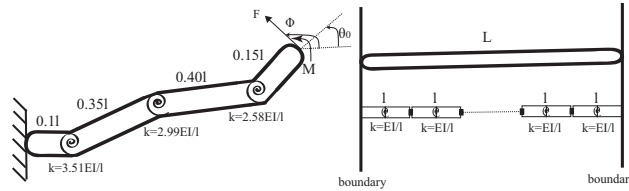


Figure 16: The PRB-3R model (left) and the finite segment model (right) for compliant beams.

Recently, Venkiteswaran and Su [56] proposed a uniform way of representing different PRB models with a matrix called a PRB matrix:

$$\Omega = \begin{bmatrix} \gamma_1 & k_{ex1} & k_{\theta1} \\ \dots & \dots & \dots \\ \gamma_n & k_{exn} & k_{\theta n} \end{bmatrix} \quad (6)$$

where each row represents a different segment in the flexible beam. Each row consists of length of the segment(γ), torsion spring(k_{ex}) and the flexibility of the spring($k_{\theta n}$). This representation of compliant beams is adopted in the software and each individual flexible beam can be represented with a predefined but customizable PRB matrix.

Kinetostatic analysis is to determine the deflection of a compliant mechanism upon a given load or vice versa. To derive kinetostatic equations (coupled kinematic and static equilibrium), several methods for derivation of kinetostatic formulation exist. Direct stiffness approach [57–59] can be used to perform linear static analysis. This method is currently being used in static analysis of rigid-body (SAM [45]) and compliant mechanisms (CoMeT [47]). Although it has advantage of simple formulation, the stiffness approach is based on linear models, hence not accurate for large deflections.

On the other hand, energy methods [60] can be used for nonlinear static analysis. Virtual work principle was employed to calculate deformation of parallel mechanisms [61, 62]. Optimization of potential energy has been used for a wide variety of applications from molecular mechanics [63] to human walking [64]. In this task, we implemented the energy based approach for formulation of kinetostatic equations. A stationary potential energy is the necessary and sufficient condition for equilibrium of a conservative system. This means that equilibrium position (stationary) point can be obtained from minimization of the potential energy function and work for external forces or moments. Furthermore, this optimization is also subject to the kinematic constraint defined in Eq.(3). In summary, the optimization problem to be solved is mathematically formulated as:

$$\begin{aligned} \min_{\psi_i} f = & \left(\sum_{k=1}^n \frac{1}{2} k_i \psi_k^2 - \sum_{i=0}^n \int_{r_{i0}}^{r_i} \vec{F}_i \cdot d\vec{r} - \sum_{j=0}^m \int_{\theta_{j0}}^{\theta_j} M_j d\theta \right) \\ \text{subject to } g = & \sum_{i=1}^n C_{ki} \vec{Z}_i = 0 \end{aligned} \quad (7)$$

where (k_i, ψ_i) equals to (k_e, x) and (k_θ, θ) for linear and torsion springs, respectively.

Summary of Main Results This task resulted in DAS 2D [65], a conceptual design tool for planar compliant mechanisms. The compliant mechanism design software is implemented in MATLAB using object oriented programming by taking advantage of the built-in nonlinear equation solver, optimizer and plotting tools. Also graphical user interfaces have been implemented to facilitate the design process. We developed five different analysis modules (Fig. 17) capable of kinematic and kinetostatic analysis of mechanisms.

Static force analysis is to determine the relationship between the deflection of a compliant mechanism and the external load applied upon. The module starts with converting compliant links into a series of rigid-body links using pseudo-rigid-body model described earlier. Then, kinematic equations are derived based on the independent kinematic loops. Afterwards, a breadth-first search algorithm is used to determine the deflection of the point where the external force is applied. Finally the optimizer in Eq.(7) is employed in the last optimization step for the static analysis.

Opposite to the static force analysis, the distance analysis is to determine the required load(s) that will result in a prescribed deformation. The desired deformation can be translation of a node or rotation of a link and the output of the module will be the magnitudes of the loads exerting at a given position.

Mechanical advantage is defined as the ratio of the output force/moment over the input force/moment. It is one of the most important design criterion in compliant mechanisms. Mechanical advantage analysis is to find the balancing load for a given input load.

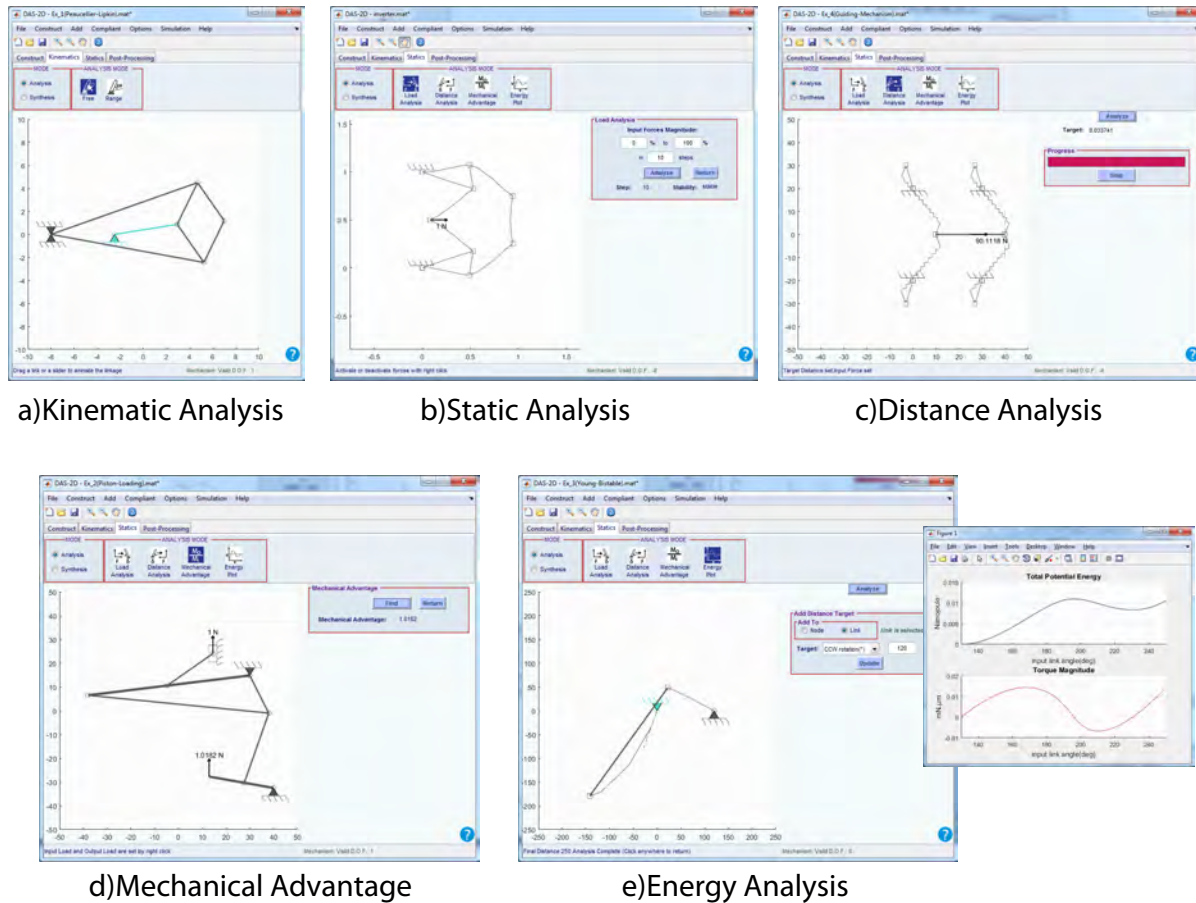


Figure 17: Five different analysis modules are shown.

The energy/torque vs. the input load curve gives the designer a visualized way to evaluate the quality of a compliant mechanism. The energy analysis module plots the distance versus load and energy graph until a desired deflection.

6 DAS-2D: Kinetostatic Synthesis of Planar Compliant Mechanisms

Objective: In this task, we extend the capabilities of the DAS 2D mechanism simulation software that allows users to perform kinematic and kinetostatic synthesis. Geometric properties and compliances of the flexible members are synthesized for predefined kinematic and static requirements during the kinetostatic synthesis. Earlier, we had developed the object oriented planar mechanism analysis tool and this study expands the capabilities of DAS 2D software to include interactive kinematic synthesis. We also present a solver that enables users to access and use main analysis classes of the software. These classes can be used for custom analysis and synthesis cases and can be integrated to other software programs.

Methodology: Kinematic synthesis is a systematic attempt to calculate the design variables of a mechanism in order to achieve the desired function. Static analysis should be combined with the kinematic analysis to reveal the relationship between the design loads and the accompanying deflection of a compliant mechanism. This relation can be employed in kinetostatic analysis of compliant mechanisms for obtaining the desired relation between the input and output loads and the resulting deflections.

There are a number of software programs available for kinematic synthesis of mechanisms. These tools' capabilities are mostly limited to few mechanism types. Linkages [66] is capable of planar four bar, five bar and six bar mechanism synthesis and planar mechanism synthesis with Sphinx [67] is restricted to mechanisms with four pin joints. Similarly, kinematic synthesis with six pin joints is possible [68]. Serial chain spatial mechanism synthesis is available with Synthetica [69] and likewise, Spades [70] can be used for spatial mechanisms consisting of four cylindrical joints. Parallel manipulators with RRR and RPR legs can also be synthesized [71]. SAM [45] is a commercial mechanism design tool and is capable of kinematic synthesis of planar mechanisms. Ch Mechanism Toolkit [72] enables users to create and analyze specific mechanisms with the Ch language. Kinematic synthesis can be achieved by developing case by case synthesis codes. Yu et. al. [50] also developed a kinematic synthesis tool that can synthesize a mechanism that will trace the input coupler curve. However, the solver is limited to the mechanisms that are stored in their database.

No software tool is available for synthesis of compliant mechanisms, although the fundamental theory has been developed for some time. Topology optimization [73, 74] and kinetostatic synthesis [75] are the two principal kinetostatic synthesis techniques for compliant mechanisms. Topology optimization, which is more suited to truss type mechanisms, employs finite element methods to minimize the total strain energy of the structure. Kinetostatic synthesis methods convert the compliant mechanism to rigid body mechanisms via pseudo-rigid-body models (PRBM) [30] and solve the synthesis problem using the resulting rigid body mechanism.

We previously developed a graphical mechanism simulation tool [65, 76] capable of unified design and analysis of planar rigid and compliant mechanisms. As a next step, interactive kinematic and kinetostatic synthesis capabilities were developed. The software is developed with MATLAB employing complete object oriented approach. Fig. 18 demonstrate the design, analysis and synthesis classes of the software. The graphical user interface has access to all three class groups and provides interactive design, analysis and synthesis of mechanisms. We also developed a solver program that allows users to integrate design and analysis classes to other MATLAB applications. These classes allow users to easily create and analyze any planar mechanism with a few line of codes. Therefore, the solver broadens the capability of software to the complex cases beyond the user interface. This paper presents the interactive synthesis modules and the solver.

The kinematic synthesis problem is defined as matching the coupler curve of a designed mechanism with a desired coupler curve. Type-P [77] and Type-Z [78] are two similar methods for calculating the Fourier descriptors of closed or open curves. Type-P descriptors are calculated using exact positions of the points on a curve and on the other hand, Type-Z descriptors utilize the slope between every two points on the curve. Type-P descriptors are sensitive to scaling, rotation and translation resulting in difficulty in converging to the optimal solution. A point and the corresponding slope on a curve are defined as:

$$\mathbf{p}_i = x_i + iy_i \quad i=1, \dots, n \quad \mathbf{s}_i = \frac{p_{i+1} - p_i}{||p_{i+1} - p_i||} \quad i=1, \dots, n-1 \quad (8)$$

where n is the number of points on the curve.

Type-P descriptors can be calculating based on previously defined slope information:

$$F.D.k = \frac{1}{n} \sum_{j=0}^{n-1} s_j \exp \left(-2\pi i \frac{jk}{n} \right) - N \leq k \leq N \quad (9)$$

where N determines the accuracy of the curve representation.

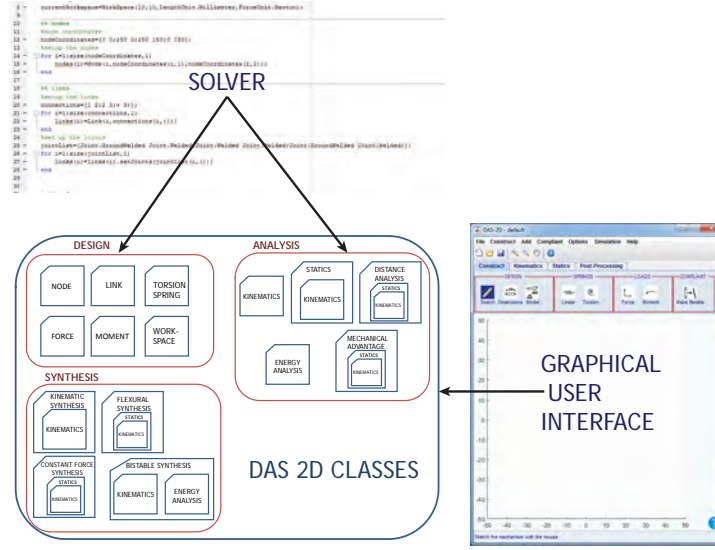


Figure 18: The structure of the DAS 2D program.

With the Type-P descriptors, the kinematic synthesis problem can be defined as an constrained optimization problem:

$$\min_{\psi_i} f = \left(\sum_{i=1}^{2N+1} \|F.D.i(\gamma_T) - F.D.i(\gamma_C)\| \right) \quad (10)$$

subject to *Optimization Boundary*

where ψ_i are the link lengths.

Since Eqs.(8-10) are not sensitive to curve translation, rotation and scaling, the resulting mechanism must be post-processed. Rotation and scaling can lead to mechanism moving out the optimization boundary but the size of the mechanism will not be altered. However, the scaling operation will definitely modify the size of the optimized mechanism. The scaling operation will be highly undesirable if a very small part of the coupler curve traces the target open curve and the resulting mechanism will be much larger than the optimization boundary. Due to this undesirable scaling in open curves, the slope in Eq.(8) is modified as:

$$s_i = p_{i+1} - p_i \quad i=1, \dots, n-1 \quad (11)$$

With this modification, the Type-P transform will be sensitive to scaling operation and therefore, the optimized mechanism does not need to be scaled after optimization.

A kinetostatic synthesis case arises when loads acting on the mechanism are known and a specific deflection is desired. In this case, the role of the tool is determining the cross-section (I) and material (E) properties of the flexible members in the mechanism. In this case, overall design of the mechanism is known but the flexural stiffnesses (EI) of the compliant members are unknown. Therefore, the number of unknowns are equal to the number of compliant members. The synthesis problem can be converted to the following optimization problem:

$$\min_{EI} f = (\Delta_{des} - \Delta_{cur}(EI)) \quad (12)$$

Bistable mechanisms are special kind of mechanisms that have two equilibrium points. The mechanism will stay at these points without requiring any external force. Compliant bistable mechanisms acquire two stable states by storing energy at their compliant segments. Critical load is defined as the maximum external load (force or moment) that is required to actuate the mechanism from one stable to the other stable position. We can define two different synthesis cases for bistable mechanisms. First synthesis mode (Optimization Variables: EI_i , Eq.(13) is for finding the required stiffness(es) for the compliant beam(s) that will result in specified critical load.

$$\min_{EI} f = (C.L_{des} - C.L_{cur}(EI)) \quad (13)$$

Alternatively, in the second synthesis (Optimization Variables: $node(x_i, y_i)$, Eq.(14) desired instable and stable positions of the mechanism can be determined and the link lengths can be found via optimization. First synthesis mode is a kinetostatic synthesis problem, whereas the second synthesis mode is a kinematic synthesis problem.

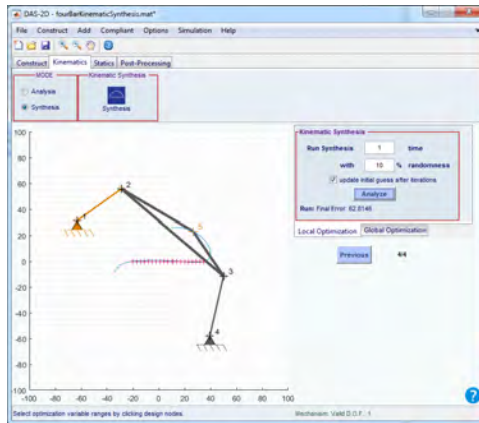
$$\min_{node(x,y)} f = (S.P_{des} - S.P_{cur}(node(x, y))) \quad (14)$$

Constant force mechanisms are the mechanisms that maintain a constant output force during a deflection range. Compliant members or compliant joints can also be used in a constant force mechanism. For a compliant mechanism, the link length, torsional spring stiffness and flexural stiffness ratios must be established in a way that the load output of the mechanism will be almost constant. The optimization (Eq.(15) problem can be stated as:

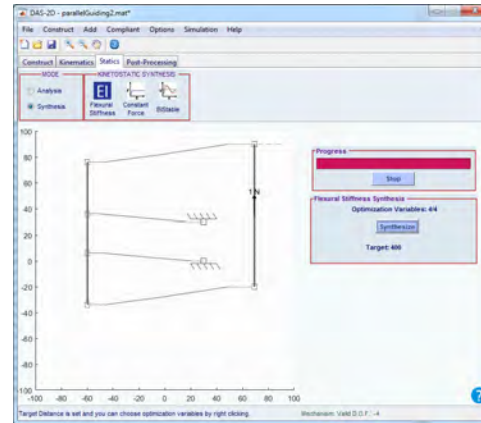
$$\begin{aligned} \min_{R_i} f &= \left(\frac{F_{max}(R_i)}{F_{min}(R_i)} \right) \\ &\text{subject to } lb_i \leq R_i \leq ub_i \end{aligned} \quad (15)$$

Summary of Main Results The capabilities of the DAS 2D early design tool has been extended to compliant mechanism synthesis. There are four (Fig. 19) synthesis modules that are capable of kinematic and kinetostatic synthesis of compliant mechanisms. Kinematic synthesis module will match the current coupler curve of a mechanism to a desired curve. Kinetostatic synthesis module will find the required flexural stiffnesses of compliant members that will result in the prescribed deflection. Bistable mechanism synthesis module modifies the bistable behavior of a bistable mechanism. Constant force mechanism will alter the design of a mechanism in order to have a constant force output.

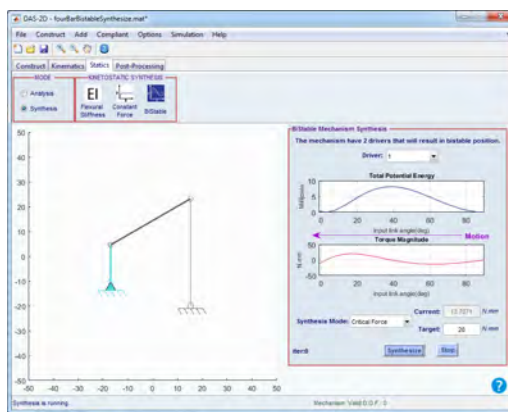
In addition to the synthesis modules, a solver that can be integrated to MATLAB is developed. This solver enables developers to access the design and analysis classes directly in MATLAB and by this way, the developers can utilize the classes in their codes to develop custom analysis or synthesis methods for compliant mechanisms.



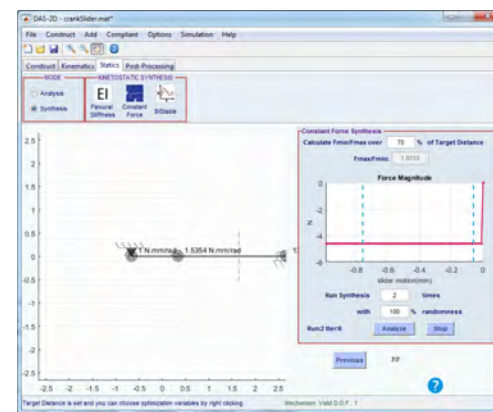
a) Kinematic Synthesis



b) Kinetostatic Synthesis



c) Bistable Mechanism Synthesis



d) Constant Mechanism Synthesis

Figure 19: Four different synthesis modules are shown.

References

- [1] Tsai, L.-W., 2000. *Mechanism Design: Enumeration of Kinematic Structures According to Function*. CRC Press LLC, New York, NY.
- [2] Murphy, M. D., 1993. "A generalized theory for the type synthesis and design of compliant mechanisms". Phd thesis, Purdue University, West Lafayette, IN.
- [3] Zupan, M., 2002. "Actuator classification and selection-the development of a database". *Advanced Engineering Materials*, **4**, pp. 933–940.
- [4] Bell, D. J., Lu, T. J., Fleck, N. A., and Spearing, S. M., 2005. "MEMS actuators and sensors: observations on their performance and selection for purpose". *Journal of Micromechanics and Microengineering*, **15**(7), July, pp. S153–S164.
- [5] Conn, A. T., Burgess, S. C., and Ling, C. S., 2007. "Design of a parallel crank-rocker flapping mechanism for insect-inspired micro air vehicles". *Proceedings of the Institution of Mechanical Engineers, Part C: Journal of Mechanical Engineering Science*, **221**(10), pp. 1211–1222.
- [6] Conn, A., Burgess, S., Hyde, R., and Ling, C. S., 2006. "From natural flyers to the mechanical realization of a flapping wing micro air vehicle". In *IEEE International Conference on Robotics and Biomimetics, 2006. ROBIO '06*, IEEE, pp. 439–444.

- [7] Klaptocz, A., Nicoud, J.-D., Floreano, D., Zufferey, J.-C., Srinivasan, M., and Ellington, C., 2010. “Technology and fabrication of ultralight micro-aerial vehicles”. In *Flying Insects and Robots*. Springer Berlin Heidelberg, pp. 299–316.
- [8] Bolsman, C., 2010. “Flapping wing actuation using resonant compliant mechanisms: An insect-inspired design”. *Doctoral Thesis*, Oct.
- [9] Gerdes, J. W., Gupta, S. K., and Wilkerson, S. A., 2010. “A review of bird-inspired flapping wing miniature air vehicle designs”. *ASME Conference Proceedings*, **2010**(44106), pp. 57–67.
- [10] Keennon, M., Klingebiel, K., Won, H., and Andriukov, A., 2012. “Development of the nano hummingbird: A tailless flapping wing micro air vehicle”. In 50th AIAA Aerospace Sciences Meeting including the New Horizons Forum and Aerospace Exposition.
- [11] Steltz, E., Avadhanula, S., and Fearing, R., 2007. “High lift force with 275 hz wing beat in mfi”. In *Intelligent Robots and Systems, 2007. IROS 2007. IEEE/RSJ International Conference on*, pp. 3987–3992.
- [12] Avadhanula, S., Wood, R. J., Campolo, D., and Fearing, R. S., 2002. “Dynamically tuned design of the MFI thorax”. In *IEEE International Conference on Robotics and Automation, 2002. Proceedings. ICRA ’02, Vol. 1, IEEE*, pp. 52–59 vol.1.
- [13] Avadhanula, S., Wood, R. J., Steltz, E., Yan, J., and Fearing, R. S., 2003. “Lift force improvements for the micromechanical flying insect”. In *2003 IEEE/RSJ International Conference on Intelligent Robots and Systems, 2003. (IROS 2003). Proceedings, Vol. 2, IEEE*, pp. 1350–1356 vol.2.
- [14] Galiski, C., and bikowski, R., 2005. “Insect-like flapping wing mechanism based on a double spherical scotch yoke”. *Journal of The Royal Society Interface*, **2**(3), June, pp. 223–235.
- [15] Fenelon, M. A. A., 2009. “Biomimetic flapping wing aerial vehicle”. In *Proceedings of the 2008 IEEE International Conference on Robotics and Biomimetics, IEEE Computer Society*, pp. 1053–1058.
- [16] Lentink, D., Jongerius, S. R., and Bradshaw, N. L., 2009. “The scalable design of flapping micro-air vehicles inspired by insect flight”. In *Flying Insects and Robots*, D. Floreano, J.-C. Zufferey, M. V. Srinivasan, and C. Ellington, eds. Springer Berlin Heidelberg, Berlin, Heidelberg, pp. 185–205.
- [17] de Croon, G., de Clercq, K., Ruijsink, Ruijsink, R., Remes, Remes, B., and de Wagter, C., 2009. “Design, aerodynamics, and vision-based control of the DelFly”. *International Journal of Micro Air Vehicles*, **1**(2), June, pp. 71–97.
- [18] Sc, B. B. B., 2010. “Improving flight performance of DelFly II in hover by improving wing design and driving mechanism”. *Master Thesis*.
- [19] Wood, R. J., 2008. “The first takeoff of a biologically inspired at-scale robotic insect”. *IEEE Transactions on Robotics*, **24**(2), Apr., pp. 341–347.
- [20] Sreetharan, P. S., and Wood, R. J., 2010. “Passive aerodynamic drag balancing in a flapping-wing robotic insect”. *ASME Journal of Mechanical Design*, **132**(5), May, pp. 051006–11.

- [21] Sreetharan, P., and Wood, R., 2011. “Passive torque regulation in an underactuated flapping wing robotic insect”. *Autonomous Robots*, **31**(2), Oct., pp. 225–234.
- [22] Nguyen, Q. V., Park, H. C., Goo, N. S., and Byun, D., 2008. “Flapping performance and simulation of an insect-mimicking flapper actuated by a compressed unimorph piezoelectric composite actuator”. In *Active and Passive Smart Structures and Integrated Systems 2008*, M. Ahmadian, ed., Vol. 6928, SPIE, pp. 69281N–12.
- [23] Madangopal, R., Khan, Z. A., and Agrawal, S. K., 2005. “Biologically inspired design of small flapping wing air vehicles using Four-Bar mechanisms and quasi-steady aerodynamics”. *Journal of Mechanical Design*, **127**(4), July, pp. 809–816.
- [24] Bejgerowski, W., Gerdes, J. W., Gupta, S. K., Bruck, H. A., and Wilkerson, S., 2010. “Design and fabrication of a multi-material compliant flapping wing drive mechanism for miniature air vehicles”. *ASME Conference Proceedings*, **2010**(44106), Jan., pp. 69–80.
- [25] Bejgerowski, W., Ananthanarayanan, A., Mueller, D., and Gupta, S. K., 2009. “Integrated product and process design for a flapping wing drive mechanism”. *ASME Journal of Mechanical Design*, **131**(6), June, pp. 061006–9.
- [26] Keennon, M., Klingebiel, K., Won, H., and Andriukov, A., 2012. “Development of the Nano Hummingbird: A Tailless Flapping Wing Micro Air Vehicle”. In *50th AIAA Aerospace Sciences Meeting including the New Horizons Forum and Aerospace Exposition*.
- [27] Howell, L. L., 2001. *Compliant mechanisms*. Wiley-Interscience.
- [28] Theodoresen, T., 1935. General theory of aerodynamic instability and mechanism of flutter. Tech. Rep. 496, NACA.
- [29] Howell, L. L., and Midha, A., 1994. “A Method for the Design of Compliant Mechanisms With Small-Length Flexural Pivots”. *Journal of Mechanical Design*, **116**(1), Mar., pp. 280–290.
- [30] Howell, L. L., and Midha, A., 1995. “Parametric Deflection Approximations for End-Loaded, Large-Deflection Beams in Compliant Mechanisms”. *Journal of Mechanical Design*, **117**(1), Mar., pp. 156–165.
- [31] Dado, M. H., 2001. “Variable parametric pseudo-rigid-body model for large-deflection beams with end loads”. *International Journal of Non-Linear Mechanics*, **36**(7), Oct., pp. 1123–1133.
- [32] Su, H.-J., 2009. “A Pseudorigid-Body 3r Model for Determining Large Deflection of Cantilever Beams Subject to Tip Loads”. *Journal of Mechanisms and Robotics*, **1**(2), Jan., pp. 021008–021008.
- [33] Vogtmann, D. E., Gupta, S. K., and Bergbreiter, S., 2013. “Characterization and Modeling of Elastomeric Joints in Miniature Compliant Mechanisms”. *Journal of Mechanisms and Robotics*, **5**(4), Oct., pp. 041017–041017.
- [34] Timoshenko, S., 1921. “On the correction for shear of the differential equation for transverse vibrations of prismatic bars”. *Philosophical Magazine Series 6*, **41**(245), pp. 744–746.
- [35] Timoshenko, S., 1922. “On the transverse vibrations of bars of uniform cross-section”. *Philosophical Magazine Series 6*, **43**(253), pp. 125–131.

- [36] Chen, G., Xiong, B., and Huang, X., 2011. “Finding the optimal characteristic parameters for 3r pseudo-rigid-body model using an improved particle swarm optimizer”. *Precision Engineering*, **35**(3), July, pp. 505–511.
- [37] Yu, Y.-Q., Feng, Z.-L., and Xu, Q.-P., 2012. “A pseudo-rigid-body 2r model of flexural beam in compliant mechanisms”. *Mechanism and Machine Theory*, **55**, Sept., pp. 18–33.
- [38] Pei, X., Yu, J., Zong, G., and Bi, S., 2010. “An effective pseudo-rigid-body method for beam-based compliant mechanisms”. *Precision Engineering*, **34**(3), July, pp. 634–639.
- [39] Saxena, A., and Kramer, S. N., 1998. “A Simple and Accurate Method for Determining Large Deflections in Compliant Mechanisms Subjected to End Forces and Moments”. *Journal of Mechanical Design*, **120**(3), Sept., pp. 392–400.
- [40] Vogtmann, D., Gupta, S. K., and Bergbreiter, S., 2013. “Modeling and Optimization of a Miniature Elastomeric Compliant Mechanism Using a 3-Spring Pseudo Rigid Body Model”. In *37th Mechanisms and Robotics Conference*, Vol. 6A.
- [41] Howell, L. L., Magleby, S. P., and Olsen, B. M., 2013. *Handbook of Compliant Mechanisms*. John Wiley & Sons, Jan.
- [42] Howell, L. L., Midha, A., and Norton, T. W., 1996. “Evaluation of Equivalent Spring Stiffness for Use in a Pseudo-Rigid-Body Model of Large-Deflection Compliant Mechanisms”. *Journal of Mechanical Design*, **118**(1), Mar., pp. 126–131.
- [43] Edwards, B. T., Jensen, B. D., and Howell, L. L., 1999. “A Pseudo-Rigid-Body Model for Initially-Curved Pinned-Pinned Segments Used in Compliant Mechanisms”. *Journal of Mechanical Design*, **123**(3), June, pp. 464–468.
- [44] Paul, B., 1979. *Kinematics and Dynamics of Planar Machinery*. Prentice-Hall.
- [45] Rankers, A. M., and Schrama, H. W., 2002. “SAM: Simulation and Analysis of Mechanisms”. In *ASME 2002 International Design Engineering Technical Conferences and Computers and Information in Engineering Conference*, American Society of Mechanical Engineers, pp. 1383–1387.
- [46] Petri, P. A., 2002. “A continuum mechanic design aid for non-planar compliant mechanisms”. PhD thesis, Massachusetts Institute of Technology.
- [47] Culpepper, M. L., and Kim, S., 2004. “A Framework and Design Synthesis Tool Used to Generate, Evaluate and Optimize Compliant Mechanism Concepts for Research and Education Activities”. *ASME 2004 International Design Engineering Technical Conferences and Computers and Information in Engineering Conference*, **2**, Jan., pp. 1583–1588.
- [48] Yu, W., and Blair, M., 2012. “GEBT: A general-purpose nonlinear analysis tool for composite beams”. *Composite Structures*, **94**(9), Sept., pp. 2677–2689.
- [49] Jonker, J. B., and Meijaard, J. P., 1990. “SPACARComputer program for dynamic analysis of flexible spatial mechanisms and manipulators”. In *Multibody systems handbook*. Springer, pp. 123–143.
- [50] Yue, C., Su, H.-J., and Ge, Q. J., 2012. “A hybrid computer-aided linkage design system for tracing open and closed planar curves”. *Computer-Aided Design*, **44**(11), Nov., pp. 1141–1150.

- [51] MSC Software. Adams, <http://www.mscsoftware.com/product/adams>.
- [52] Dobrjanskyj, L., and Freudenstein, F., 1967. "Some Applications of Graph Theory to the Structural Analysis of Mechanisms". *Journal of Manufacturing Science and Engineering*, **89**(1), Feb., pp. 153–158.
- [53] Chen, D.-Z., and Lin, T.-W., 1998. "Dynamic analysis of geared robotic mechanisms using graph theory". *Journal of Mechanical Design*, **120**, p. 241.
- [54] Shi, P., and McPhee, J., 2000. "Dynamics of Flexible Multibody Systems Using Virtual Work and Linear Graph Theory". *Multibody System Dynamics*, **4**(4), Nov., pp. 355–381.
- [55] Freudenstein, F., and Maki, E., 1979. "The creation of mechanisms according to kinematic structure and function". *Environment and Planning B*, **6**(4), pp. 375–391.
- [56] Venkiteswaran, V. K., and Su, H.-J., 2014. "A parameter optimization framework for determining the pseudo-rigid-body model of cantilever-beams". *Precision Engineering*.
- [57] Melosh, R. J., 1963. "Basis for derivation of matrices for the direct stiffness method". *AIAA Journal*, **1**(7), pp. 1631–1637.
- [58] Hughes, T. J., 2012. *The finite element method: linear static and dynamic finite element analysis*. Courier Dover Publications.
- [59] Ranzi, G., Bradford, M. A., and Uy, B., 2004. "A direct stiffness analysis of a composite beam with partial interaction". *International Journal for Numerical Methods in Engineering*, **61**(5), pp. 657–672.
- [60] Reddy, J. N., 2002. *Energy Principles and Variational Methods in Applied Mechanics*. John Wiley & Sons, Aug.
- [61] Xiangzhou, Z., Yougao, L., Zhiyong, D., and Hongzan, B., 2007. "Statics of rotational 3-UPU parallel mechanisms based on principle of virtual work". In IEEE International Conference on Robotics and Biomimetics, 2007. ROBIO 2007, pp. 1954–1959.
- [62] Jess Cervantes-Snchez, J., Rico-Martnez, J. M., Pacheco-Gutierrez, S., and Cerda-Villafaa, G., 2012. "Static analysis of spatial parallel manipulators by means of the principle of virtual work". *Robotics and Computer-Integrated Manufacturing*, **28**(3), June, pp. 385–401.
- [63] Pillardy, J., Czaplewski, C., Liwo, A., Lee, J., Ripoll, D. R., Kamierkiewicz, R., O\ldziej, S., Wedemeyer, W. J., Gibson, K. D., Arnautova, Y. A., Saunders, Jeff, Ye, Yuan-Jie, and Scheraga, Harold A., 2001. "Recent improvements in prediction of protein structure by global optimization of a potential energy function". *Proceedings of the National Academy of Sciences*, **98**(5), pp. 2329–2333.
- [64] Zarrugh, M. Y., Todd, F. N., and Ralston, H. J., 1974. "Optimization of energy expenditure during level walking". *European Journal of Applied Physiology and Occupational Physiology*, **33**(4), Dec., pp. 293–306.
- [65] DISL. DAS Software, <http://www.compliantanalysis.com>.
- [66] Norton Associates Engineering. Linkages, <http://www.designofmachinery.com/Linkage/>.

- [67] Larochelle, P. M., Dooley, J., Murray, A. P., and McCarthy, J. M., 1993. “Sphinx: Software for synthesizing spherical 4r mechanisms”. In NSF Design and Manufacturing Systems Conference, Vol. 1, pp. 607–611.
- [68] Wu, J., Purwar, A., and Ge, Q. J., 2010. “Interactive Dimensional Synthesis and Motion Design of Planar 6r Single-Loop Closed Chains via Constraint Manifold Modification”. *Journal of Mechanisms and Robotics*, **2**(3), July, pp. 031012–031012.
- [69] Perez, A., Su, H.-J., and McCarthy, J. M., 2004. “Synthetica 2.0: software for the synthesis of constrained serial chains”. In ASME 2004 International Design Engineering Technical Conferences and Computers and Information in Engineering Conference, American Society of Mechanical Engineers, pp. 1363–1369.
- [70] Larochelle, P., 1998. “Spades: software for synthesizing spatial 4c mechanisms”. In Proceedings of the ASME 1998 Design Engineering Technical Conferences and Computers and Information Conference.
- [71] Purwar, A., and Gupta, A., 2011. “Visual Synthesis of RRR- and RPR-Legged Planar Parallel Manipulators Using Constraint Manifold Geometry”. pp. 1081–1092.
- [72] Cheng, H. H., and Trang, D. T., 2005. “Object-oriented interactive mechanism design and analysis”. *Engineering with Computers*, **21**(3), Dec., pp. 237–246.
- [73] Frecker, M. I., Ananthasuresh, G. K., Nishiwaki, S., Kikuchi, N., and Kota, S., 1997. “Topological Synthesis of Compliant Mechanisms Using Multi-Criteria Optimization”. *Journal of Mechanical Design*, **119**(2), June, pp. 238–245.
- [74] Pedersen, C. B. W., Buhl, T., and Sigmund, O., 2001. “Topology synthesis of large-displacement compliant mechanisms”. *International Journal for Numerical Methods in Engineering*, **50**(12), pp. 2683–2705.
- [75] Howell, L. L., and Midha, A., 1996. “A Loop-Closure Theory for the Analysis and Synthesis of Compliant Mechanisms”. *Journal of Mechanical Design*, **118**(1), Mar., pp. 121–125.
- [76] Turkkan, O. A., and Su, H.-J., 2014. “A Unified Kinetostatic Analysis Framework for Planar Compliant and Rigid Body Mechanisms”. In ASME 2014 International Design Engineering Technical Conferences and Computers and Information in Engineering Conference, American Society of Mechanical Engineers, pp. V05BT08A090–V05BT08A090.
- [77] Zahn, C. T., and Roskies, R. Z., 1972. “Fourier Descriptors for Plane Closed Curves”. *IEEE Transactions on Computers*, **21**(3), pp. 269–281.
- [78] Uesaka, Y., 1984. “A new fourier descriptor applicable to open curves”. *Electronics and Communications in Japan (Part I: Communications)*, **67**(8), Jan., pp. 1–10.

Table 2: Type Synthesis of Flapping Mechanisms I


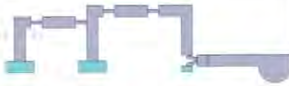
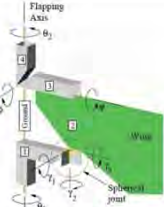

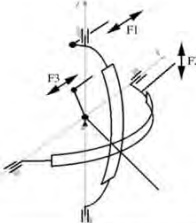
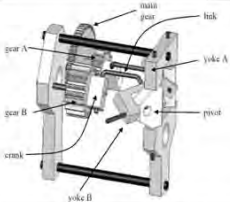

Research Group	Project	Kinematic Diagram	Adjacency Matrix	Characteristic Polynomial Coeff.
Aero-Vironment	Nano Hummingbird		$\begin{bmatrix} -1 & 1 & 0 & 0 & 1 & 0 & 0 & 1 \\ 1 & 0 & 1 & 0 & 0 & 0 & 0 & 0 \\ 0 & 1 & C & 1 & 0 & 0 & 0 & 0 \\ 0 & 0 & 1 & C & 1 & 0 & 0 & 0 \\ 1 & 0 & 0 & 1 & 1 & 0 & 0 & 5 \\ 0 & 0 & 0 & 0 & 0 & C & 1 & 0 \\ 0 & 0 & 0 & 0 & 0 & 1 & C & 1 \\ 1 & 0 & 0 & 0 & 5 & 0 & 1 & 0 \end{bmatrix}$	$\begin{aligned} C_8 &= 1 \\ C_7 &= -4C \\ C_6 &= -34 + 6C^2 \\ C_5 &= -34 + 129C - 4C^3 \\ C_4 &= 123 + 135C - 185C^2 + C^4 \\ C_3 &= 100 - 324C - 201C^2 + 119C^3 \\ C_2 &= -128 - 232C + 310C^2 + 133C^3 - 29C^4 \\ C_1 &= -64 + 162C + 165C^2 - 133C^3 - 33C^4 \\ C_0 &= 36 + 32C - 64C^2 - 33C^3 + 25C^4 \end{aligned}$
Berkeley	MFI		$\begin{bmatrix} -1 & 2 & 0 & 2 & 0 & 2 \\ 1 & 0 & 2 & 0 & 0 & 0 \\ 0 & 2 & 0 & 2 & 0 & 0 \\ 1 & 0 & 2 & 0 & 2 & 0 \\ 0 & 0 & 0 & 2 & 0 & 2 \\ 1 & 0 & 0 & 0 & 2 & 0 \end{bmatrix}$	$\begin{aligned} C_6 &= 1 \\ C_5 &= 1 \\ C_4 &= -22 \\ C_3 &= -16 \\ C_2 &= 80 \\ C_1 &= 48 \\ C_0 &= -32 \end{aligned}$
	Wing Differential I		$\begin{bmatrix} -1 & 1 & 0 & 0 & 1 \\ 1 & 0 & 2 & 0 & 0 \\ 0 & 2 & 0 & 2 & 0 \\ 0 & 0 & 2 & 0 & 2 \\ 1 & 0 & 0 & 2 & 0 \end{bmatrix}$	$\begin{aligned} C_5 &= -1 \\ C_4 &= -1 \\ C_3 &= 14 \\ C_2 &= 12 \\ C_1 &= -32 \end{aligned}$
	Wing Differential II		$\begin{bmatrix} -1 & 1 & 0 & 0 & 1 \\ 1 & 0 & 2 & 0 & 0 \\ 0 & 2 & 0 & 2 & 0 \\ 0 & 0 & 2 & 0 & 2 \\ 1 & 0 & 0 & 2 & 0 \end{bmatrix}$	$\begin{aligned} C_5 &= -1 \\ C_4 &= -1 \\ C_3 &= 14 \\ C_2 &= 12 \\ C_1 &= -32 \end{aligned}$
Warsaw University of Technology & Cranfield University	Lissajous MAV		$\begin{bmatrix} -1 & 1 & 0 & 1 & 1 \\ 1 & 0 & 6 & 0 & 0 \\ 0 & 6 & 0 & 7 & 7 \\ 1 & 0 & 7 & Y & 0 \\ 1 & 0 & 7 & 0 & Y \end{bmatrix}$	$\begin{aligned} C_5 &= -1 \\ C_4 &= -1 + 2Y \\ C_3 &= 137 + 2Y - Y^2 \\ C_2 &= 134 - 174Y - Y^2 \\ C_1 &= -2 - 170Y + 37Y^2 \\ C_0 &= 2Y + 36Y^2 \end{aligned}$
Defense Research Development Organization (DRDO)	VTOL MAV		$\begin{bmatrix} -1 & 1 & 0 & 6 \\ 1 & 0 & 1 & 0 \\ 0 & 1 & 0 & 1 \\ 6 & 0 & 1 & Y \end{bmatrix}$	$\begin{aligned} C_4 &= 1 \\ C_3 &= 1 - Y \\ C_2 &= -39 - Y \\ C_1 &= -2 + 2Y \\ C_0 &= 25 + Y \end{aligned}$
Konkuk University	LIPCA MAV		$\begin{bmatrix} -1 & 1 & 0 & 1 \\ 1 & 0 & 1 & 0 \\ 0 & 1 & 0 & 1 \\ 1 & 0 & 1 & 0 \end{bmatrix}$	$\begin{aligned} C_4 &= 1 \\ C_3 &= 1 \\ C_2 &= -4 \\ C_1 &= -2 \end{aligned}$

Table 3: Type Synthesis of Flapping Mechanisms II






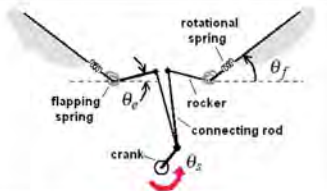
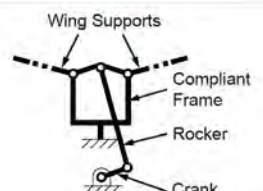
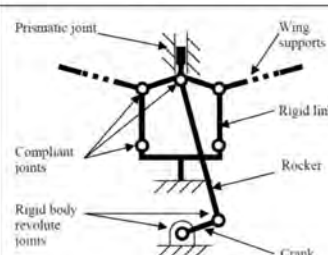
Research Group	Project	Kinematic Diagram	Adjacency Matrix	Characteristic Polynomial Coeff.
Delft University	DelFly I		$\begin{bmatrix} -1 & 1 & 0 & 1 \\ 1 & 0 & 1 & 0 \\ 0 & 1 & 0 & 1 \\ 1 & 0 & 1 & 0 \end{bmatrix}$	$\begin{aligned} c_4 &= 1 \\ c_3 &= 1 \\ c_2 &= -4 \\ c_1 &= -2 \end{aligned}$
	DelFly II & DelFly Micro		$\begin{bmatrix} -1 & 1 & 0 & 1 \\ 1 & 0 & 1 & 0 \\ 0 & 1 & 0 & 1 \\ 1 & 0 & 1 & 0 \end{bmatrix}$	$\begin{aligned} c_4 &= 1 \\ c_3 &= 1 \\ c_2 &= -4 \\ c_1 &= -2 \end{aligned}$
	New DelFly II		$\begin{bmatrix} -1 & 1 & 0 & 1 \\ 1 & 0 & 1 & 0 \\ 0 & 1 & 0 & 1 \\ 1 & 0 & 1 & 0 \end{bmatrix}$	$\begin{aligned} c_4 &= 1 \\ c_3 &= 1 \\ c_2 &= -4 \\ c_1 &= -2 \end{aligned}$
Harvard University	HMF		$\begin{bmatrix} -1 & 1 & 0 & 2 \\ 1 & 0 & 2 & 0 \\ 0 & 2 & 0 & 2 \\ 2 & 0 & 2 & 0 \end{bmatrix}$	$\begin{aligned} c_4 &= 1 \\ c_3 &= 1 \\ c_2 &= -13 \\ c_1 &= -8 \\ c_0 &= 4 \end{aligned}$
	PARiTy		$\begin{bmatrix} -1 & 1 & 0 & 0 & 2 \\ 1 & 0 & 2 & 0 & 0 \\ 0 & 2 & 0 & 2 & 0 \\ 0 & 0 & 2 & 0 & 2 \\ 2 & 0 & 0 & 2 & 0 \end{bmatrix}$	$\begin{aligned} c_5 &= -1 \\ c_4 &= -1 \\ c_3 &= 17 \\ c_2 &= 12 \\ c_1 &= -56 \\ c_0 &= 16 \end{aligned}$
University of Delaware	FWMAV		$\begin{bmatrix} -1 & 1 & 0 & 2 \\ 1 & 0 & 1 & 0 \\ 0 & 1 & 0 & 1 \\ 2 & 0 & 1 & 0 \end{bmatrix}$	$\begin{aligned} c_4 &= 1 \\ c_3 &= 1 \\ c_2 &= -7 \\ c_1 &= -2 \\ c_0 &= 1 \end{aligned}$
University of Maryland	Small Bird		$\begin{bmatrix} -1 & 1 & 0 & 0 & 3 \\ 1 & 0 & 1 & 0 & 0 \\ 0 & 1 & 0 & 1 & 0 \\ 0 & 0 & 1 & 0 & 1 \\ 3 & 0 & 0 & 1 & 1 \end{bmatrix}$	$\begin{aligned} c_5 &= -1 \\ c_4 &= 0 \\ c_3 &= 14 \\ c_2 &= 0 \\ c_1 &= -23 \\ c_0 &= 6 \end{aligned}$
	Jumbo Bird		$\begin{bmatrix} -1 & 1 & 0 & 1 & 0 & 2 \\ 1 & 0 & 1 & 0 & 0 & 0 \\ 0 & 1 & 0 & 1 & 0 & 0 \\ 1 & 0 & 1 & 0 & 2 & 0 \\ 0 & 0 & 0 & 2 & 0 & 2 \\ 2 & 0 & 0 & 0 & 2 & 0 \end{bmatrix}$	$\begin{aligned} c_6 &= 1 \\ c_5 &= 1 \\ c_4 &= -16 \\ c_3 &= -10 \\ c_2 &= 32 \\ c_1 &= 12 \\ c_0 &= -16 \end{aligned}$

Table 4: Optimization results

Objective	Constraint	Optimized variables					Optimal value	% Change
		l_1	l_4	w	α	$\Delta\theta_G$		
Max L	$P \leq 0.745W$	6mm	10mm	1mm	0.2527rad	1rad	48.95g	39.36%
Min P	$L \geq 35.12g$	3.6mm	10mm	1mm	0.2527rad	1rad	0.4044W	-45.7%
Min P	$L \geq 30g$	2.2mm	10mm	1mm	0.2527rad	1rad	0.2151W	-71.12%
Max L	$P \leq 0.8W$	6mm	9.7mm	1mm	0.2527rad	1rad	50.93g	44.99%
Max L	$P \leq 0.9W$	6mm	9.2mm	1mm	0.2527rad	1rad	54.72g	56.38%

Table 5: PRB models with 2 segments


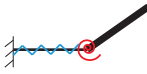

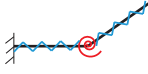
PRB model	Schematic	DOF	No. of param	Symbolic Ω	Optimal Ω	f(Ω)
1R [30]		1	2	$\begin{bmatrix} \infty & \infty & \gamma \\ k_\theta & \infty & 1 - \gamma \end{bmatrix}$	$\begin{bmatrix} \infty & \infty & 0.451 \\ 0.934 & \infty & 0.549 \end{bmatrix}$	0.0396
PR		2	3	$\begin{bmatrix} \infty & k_{ex} & \gamma \\ k_\theta & \infty & 1 - \gamma \end{bmatrix}$	$\begin{bmatrix} \infty & 0.012 & 0.441 \\ 0.942 & \infty & 0.551 \end{bmatrix}$	0.0366
RP		2	3	$\begin{bmatrix} \infty & \infty & \gamma \\ k_\theta & k_{ex} & 1 - \gamma \end{bmatrix}$	$\begin{bmatrix} \infty & \infty & 0.465 \\ 0.931 & 0.007 & 0.535 \end{bmatrix}$	0.0321
PRP [39]		3	4	$\begin{bmatrix} \infty & k_{ex1} & \gamma \\ k_\theta & k_{ex2} & 1 - \gamma \end{bmatrix}$	$\begin{bmatrix} \infty & 1.361 & 0.450 \\ 0.934 & 2.341 & 0.550 \end{bmatrix}$	0.0395

Table 6: PRB models with 3 segments


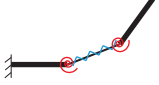
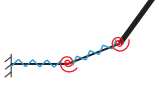
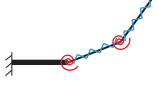

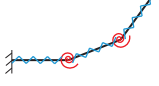


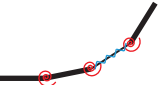
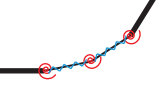
PRB model	Schematic	DOF	No. of param	Symbolic Ω	Optimal Ω	f(Ω)
2R [37]		2	4	$\begin{bmatrix} \infty & \infty & \gamma_1 \\ k_{\theta 2} & \infty & \gamma_2 \\ k_{\theta 3} & \infty & \gamma_3 \end{bmatrix}$	$\begin{bmatrix} \infty & \infty & 0.138 \\ 2.371 & \infty & 0.640 \\ 1.700 & \infty & 0.222 \end{bmatrix}$	0.0036
RPR [40]		3	5	$\begin{bmatrix} \infty & \infty & \gamma_1 \\ k_{\theta 2} & k_{ex} & \gamma_2 \\ k_{\theta 3} & \infty & \gamma_3 \end{bmatrix}$	$\begin{bmatrix} \infty & \infty & 0.139 \\ 2.369 & 3.052 & 0.639 \\ 1.701 & \infty & 0.222 \end{bmatrix}$	0.0036
PRPR		4	6	$\begin{bmatrix} \infty & k_{ex1} & \gamma_1 \\ k_{\theta 2} & k_{ex2} & \gamma_2 \\ k_{\theta 3} & \infty & \gamma_3 \end{bmatrix}$	$\begin{bmatrix} \infty & 2.987 & 0.139 \\ 2.369 & 1.778 & 0.639 \\ 1.700 & \infty & 0.222 \end{bmatrix}$	0.0035
RPRP		4	6	$\begin{bmatrix} \infty & \infty & \gamma_1 \\ k_{\theta 2} & k_{ex2} & \gamma_2 \\ k_{\theta 3} & k_{ex3} & \gamma_3 \end{bmatrix}$	$\begin{bmatrix} \infty & \infty & 0.160 \\ 2.256 & 0.099 & 0.617 \\ 1.759 & 1.082 & 0.222 \end{bmatrix}$	0.0031
PRRP		4	6	$\begin{bmatrix} \infty & k_{ex1} & \gamma_1 \\ k_{\theta 2} & \infty & \gamma_2 \\ k_{\theta 3} & k_{ex3} & \gamma_3 \end{bmatrix}$	$\begin{bmatrix} \infty & 3.096 & 0.139 \\ 2.368 & \infty & 0.639 \\ 1.701 & 3.265 & 0.222 \end{bmatrix}$	0.0035
PRPRP		4	6	$\begin{bmatrix} \infty & k_{ex1} & \gamma_1 \\ k_{\theta 2} & k_{ex2} & \gamma_2 \\ k_{\theta 3} & k_{ex3} & \gamma_3 \end{bmatrix}$	$\begin{bmatrix} \infty & 1.716 & 0.142 \\ 2.350 & 3.640 & 0.637 \\ 1.711 & 0.679 & 0.221 \end{bmatrix}$	0.0034

Table 7: PRB models with 4 segments

PRB model	Schematic	DOF	No. of param	Symbolic Ω	Optimal Ω	f(Ω)
3R [32]		3	6	$\begin{bmatrix} \infty & \infty & \gamma_1 \\ k_{\theta 2} & \infty & \gamma_2 \\ k_{\theta 3} & \infty & \gamma_3 \\ k_{\theta 4} & \infty & \gamma_4 \end{bmatrix}$	$\begin{bmatrix} \infty & \infty & 0.095 \\ 3.491 & \infty & 0.392 \\ 2.856 & \infty & 0.351 \\ 2.716 & \infty & 0.161 \end{bmatrix}$	0.0014
RPRR		4	7	$\begin{bmatrix} \infty & \infty & \gamma_1 \\ k_{\theta 2} & k_{ex2} & \gamma_2 \\ k_{\theta 3} & \infty & \gamma_3 \\ k_{\theta 4} & \infty & \gamma_4 \end{bmatrix}$	$\begin{bmatrix} \infty & \infty & 0.096 \\ 3.479 & 3.395 & 0.390 \\ 2.881 & \infty & 0.352 \\ 2.700 & \infty & 0.162 \end{bmatrix}$	0.0013
RRPR		4	7	$\begin{bmatrix} \infty & \infty & \gamma_1 \\ k_{\theta 2} & \infty & \gamma_2 \\ k_{\theta 3} & k_{ex3} & \gamma_3 \\ k_{\theta 4} & \infty & \gamma_4 \end{bmatrix}$	$\begin{bmatrix} \infty & \infty & 0.114 \\ 3.130 & \infty & 0.409 \\ 2.962 & 0.725 & 0.324 \\ 2.880 & \infty & 0.153 \end{bmatrix}$	0.0013
RPRPR		5	8	$\begin{bmatrix} \infty & \infty & \gamma_1 \\ k_{\theta 2} & k_{ex2} & \gamma_2 \\ k_{\theta 3} & k_{ex3} & \gamma_3 \\ k_{\theta 4} & \infty & \gamma_4 \end{bmatrix}$	$\begin{bmatrix} \infty & \infty & 0.108 \\ 3.359 & 3.188 & 0.385 \\ 2.828 & 0.317 & 0.353 \\ 2.827 & \infty & 0.154 \end{bmatrix}$	0.0012

1.

1. Report Type

Final Report

Primary Contact E-mail**Contact email if there is a problem with the report.**

su.298@osu.edu

Primary Contact Phone Number**Contact phone number if there is a problem with the report**

6142922239

Organization / Institution name

The Ohio State University

Grant/Contract Title**The full title of the funded effort.**

A compliant mechanism synthesis theory for fostering innovation of micro air vehicles

Grant/Contract Number**AFOSR assigned control number. It must begin with "FA9550" or "F49620" or "FA2386".**

FA9550-12-1-0070

Principal Investigator Name**The full name of the principal investigator on the grant or contract.**

Haijun Su

Program Manager**The AFOSR Program Manager currently assigned to the award**

james.fillerup@us.af.mil

Reporting Period Start Date

04/01/2012

Reporting Period End Date

03/31/2016

Abstract

In this project, we have developed a compliant mechanism synthesis theory that incorporate a general framework for determining pseudo-rigid-body models, type synthesis algorithms (determining mechanism topology for a specific task), kinetostatic analysis/synthesis. This research starts from classification and type synthesis of flapping wing MAVs. We have studied over 15 flapping mechanisms in the literature and classify them based on workspace type, linkage topology, rigid body or compliant, actuator type and mobility. This classification lays out the foundation for type synthesis of flapping wing mechanisms. We have also developed a parameter optimization framework for determining the pseudo-rigid-body (PRB) model of cantilever beams. A novel concept of "PRB matrix" has been proposed to describe the general topology of an arbitrary PRB model. A novel 3-spring pseudo-rigid-body model for soft joints with significant extension effects was proposed. These soft joints are often used in transmission mechanisms in flapping wing micro-air vehicles. Based upon this synthesis theory, we have shown that compliant joints can significantly reduce the power consumption in flapping wing MAVs if they are designed to enhance the down stroke flapping motion. We have implemented this theory into a computer-aided design software called DAS-2D with a rich user-interface. It has been applied to solve several structure design problems including design optimization of compliant transmission mechanism for flapping wing MAVs, a bistable buckling beam design and a robotic finger actuated using shape memory alloy actuators.

DISTRIBUTION A: Distribution approved for public release.

Distribution Statement

This is block 12 on the SF298 form.

Distribution A - Approved for Public Release

Explanation for Distribution Statement

If this is not approved for public release, please provide a short explanation. E.g., contains proprietary information.

SF298 Form

Please attach your [SF298](#) form. A blank SF298 can be found [here](#). Please do not password protect or secure the PDF. The maximum file size for an SF298 is 50MB.

[AFD-070820-035 -3.pdf](#)

Upload the Report Document. File must be a PDF. Please do not password protect or secure the PDF. The maximum file size for the Report Document is 50MB.

[AFOSR_FINAL_REPORT.pdf](#)

Upload a Report Document, if any. The maximum file size for the Report Document is 50MB.

Archival Publications (published) during reporting period:

Peer-reviewer journal publications:

1. Venkiteswaran V.K. and Su, H.-J., "A parameter optimization framework for determining the pseudo-rigid-body model of cantilever beams." Precision Engineering 40 (April 2015): 46–54.
doi:10.1016/j.precisioneng.2014.10.002.
2. Jonathon Cleary and Su, H.-J., "Modeling and Experimental Validation of Actuating a Bistable Buckled Beam via Moment Input." ASME Journal of Applied Mechanics. May, 2015, p.051005.
3. Venkiteswaran V.K. and Su, H.-J., "A 3-Spring Pseudo-Rigid-Body Model for Soft Joints with Significant Elongation Effects." ASME Journal of Mechanisms and Robotics, February, 2016 (in press)
4. Yu She, Chang Li, Jonathon Cleary and Su, H.-J., "Design and Fabrication of a Soft Robotic Hand with Embedded Actuators and Sensors." ASME Journal of Mechanism and Robotics., Vol. 7, no. 2, May, 2015.
5. Li, S.Z., Yu, J.J., Zong, G.H. and Su, H.-J., "A 3D Compliance-Based Approach for Designing Flexure Mechanisms that Eliminate Parasitic Errors." ASME Journal of Mechanical Design.
6. Venkiteswaran V.K. and Su, H.-J., "Extension Effects in Compliant Joints and Pseudo-Rigid-Body Models." ASME Journal of Mechanical Design, September, 2015 (under review, submitted)
7. Turkan, O.A. and Su, H.-J., "Compliant DAS-2D: A Concept Design Tool for Compliant Mechanisms." ASME Journal of Computing and Information Science in Engineering. May, 2015 (submitted, under review).

Peer-reviewer conference papers:

1. Ryan, M. and Su, H.-J., "Classification of Flapping Wing Mechanisms for Micro Air Vehicles." In: Proceedings of 2012 ASME International Design Engineering Technical Conferences. ASME. (2012): DETC2012-70953.
2. Ryan, M., Venkiteswaran V.K. and Su, H.-J., "Peak Input Torque Minimization of a Flapping Wing Mechanism for MAVs" In: Proceedings of the 54th AIAA/ASME/ASCE/AHS/ASC Structures, Structural Dynamics, and Materials Conference. (2013): AIAA-2013-1787. Boston, MA.
3. Venkiteswaran, V.K. and Su, H.-J., "Optimization of mechanism design of flapping wing MAVs" In: Proceedings of the 55th AIAA/ASME/ASCE/AHS/ASC Structures, Structural Dynamics, and Materials Conference. (2014): AIAA-2014-0573.
4. Venkiteswaran, V.K. and Su, H.-J., "Development of a 3-Spring Pseudo Rigid Body Model of Compliant Joints for Robotic Applications." In: Proceedings of ASME 2014 International Design Engineering Technical Conferences. Buffalo, NY. (2014): DETC2014-34520. (Compliant Mechanism Theory best paper award)
5. Turkan, O. A. and Su, H.-J., "A Unified Kinetostatic Analysis Framework for Planar Compliant and Rigid Body Mechanisms." In: Proceedings of ASME 2014 International Design Engineering Technical Conferences. Buffalo, NY. (2014): DETC2014-34736.
6. Venkiteswaran, V.K. and Su, H.J., "Effect of Beam Geometry on the Accuracy of Pseudo-Rigid-Body Models." In: Proceedings of ASME 2015 International Design Engineering Technical Conferences. Boston, MA. (2015): DETC201547267.

DISTRIBUTION A: Distribution approved for public release.

7. Huang, C.M. and Su, H.J, "Design of a Compliant XY Positioning Stage With Large Workspace." In: Proceedings of ASME 2015 International Design Engineering Technical Conferences. Boston, MA. (2015): DETC201547271.
8. Turkkan, O.A. and Su, H.J, "A Software for Kinetostatic Synthesis of Compliant Mechanisms." In: Proceedings of ASME 2015 International Design Engineering Technical Conferences. Boston, MA. (2015): DETC201547271.
9. She, Y., Su, H.-J., and Hurd, C., "Shape Optimization of 2D Compliant Links for Design of Inherently Safe Robots." In: Proceedings of ASME 2015 International Design Engineering Technical Conferences. Boston, MA. (2015): DETC2015-46622.

Changes in research objectives (if any):

Change in AFOSR Program Manager, if any:

The project was originally approved by Dr. David Stargel (david.stargel@afosr.af.mil). The current PM is Dr. James M. Fillerup (james.fillerup@us.af.mil)

Extensions granted or milestones slipped, if any:

The original project was extended for one year. The new end date is 03/31/2016.

AFOSR LRIR Number

LRIR Title

Reporting Period

Laboratory Task Manager

Program Officer

Research Objectives

Technical Summary

Funding Summary by Cost Category (by FY, \$K)

	Starting FY	FY+1	FY+2
Salary			
Equipment/Facilities			
Supplies			
Total			

Report Document

Report Document - Text Analysis

Report Document - Text Analysis

Appendix Documents

2. Thank You

E-mail user

Mar 14, 2016 15:39:37 Success: Email Sent to: su.298@osu.edu